Evaluation of a heated inlet to reduce humidity induced error in low-cost particulate matter sensors

Piotr Czernicki and Mathias Kallmert

LUND
UNIVERSITY

Evaluation of a heated inlet to reduce humidity induced error in low-cost particulate matter sensors

Published by
Department of Design Sciences
Faculty of Engineering LTH, Lund University
P.O. Box 118, SE-221 00 Lund, Sweden

Subject: Aerosol Technology (MAMM05)
Division: Ergonomic and Aerosol Technology
Supervisor: Erik Ahlberg
Examiner: Jakob Löndahl

Abstract

The number of low-cost particulate matter (PM) sensors available on the market has increased in recent years. They are affordable, compact and require no maintenance which means they easily can be deployed and utilized for real-time air monitoring. However, the accuracy of low-cost PM sensors has been reported to vary depending on several factors. This thesis aims to investigate and reduce errors induced by relative humidity.

Several hardware methods to reduce the relative humidity of air were considered. These include heating, diffusion, dilution and membrane drying. Heating was chosen as the most suitable method to use with low-cost PM sensors because of low maintenance, small size and low price. The chosen concept was developed into two identical prototypes consisting of a heated pipe that was attached to two Alphasense OPC-N2 sensors. To evaluate how the sensors behaved with varying humidity with and without the prototype, tests were performed in an urban environment (Malmö, Sweden). Tests in a controlled aerosol laboratory were performed as well (LTH, Lund, Sweden).

The results of the urban field test show that, when compared to the reference instrument, the native OPC-N2 sensors are susceptible to relative humidity errors especially when the RH goes above 75%. Moreover, constant offset between the two identical sensors was observed. Attachment of the heated inlet prototype improved the correlation between the OPC-N2 sensors and the reference instrument. The results of the laboratory tests were inconclusive, possibly because of the majority of the generated particles being outside the specified detection range for the low-cost PM sensors.

Keywords: particulate matter, optical particle counter, relative humidity, low-cost pm sensor, heated inlet

Sammanfattning

Partikelsensorer i den lägre prisklassen har ökat på marknaden under de senaste åren. De är prisvärda, kompakta, och kräver inget underhålll vilket innebär att de lätt kan sättas upp och användas i realtidsmätningar för olika applikationer. Mätnoggranheten på dessa sensorer har dock visats vara känslig för olika faktorer, och denna uppsats avser att utvärdera och minska felet som beror på relativ fuktighet.

I denna uppsats utvärderades flera typer av fysiska metoder för att minska den relativa luftfuktigheten. Metoder som utvärderades inkluderar uppvärmning, diffusion, utspädning och membrantorkning. Uppvärmning valdes som den mest lämpade metoden att använda då inget underhåll krävs, storleken är liten, och priset är lågt. Det utvalda konceptet utvecklades till två identiska prototyper i form av ett uppvärmt rör som fästes på två Alphasense OPC-N2. För att utfärdera påverkan av fuktighet med och utan prototypen så utfördes fälttest i stadsmiljö (Malmö, Sverige). Ett labbtest i en kontrollerad miljö utfördes också (LTH, Lund, Sverige).

Resultat från fälttesten visade att OPC-N2 visar stora mätfel speciellt när den relativa fuktigheten går över 75%. Andra observationer är att de båda sensorerna ungefärligt visar ett konstant fel mellan varandra. Påkoppling av uppvärmningsprototypen förbättrade korrelationen mellan lågkostnadssensorerna och referensinstrumentet. Labbtesterna genererade otydliga resultat, möjligen beroende på att majoriteten av de genererade partiklarna låg utom detektionsgränsen för lågkostnadssensorerna.

Nyckelord: partiklar, optisk partikelsensor, relativ fuktighet, lågkostnadspartikelsensorer, uppvärmt inlopp

Preface

This thesis was done at a company in cooperation with Ergonomics and Aerosol Technology (EAT) division of the Department of Design Sciences at LTH. The company provided us with the necessary sensors and hardware components. EAT supported us with their competence in the aerosol field and allowed us to use their laboratory equipment.

Primarily, we want to thank our supervisor Erik for guiding us in the, for us, completely new world of aerosols and for all the time he spent helping us in the lab.

We would also like to thank the team at the company who made us feel welcome, gave constructive criticism and aided in many practical steps of the prototype development.

Finally, we want to thank Mårten Spanne from Malmö Stad who helped us with the deployment of measurement boxes, provided us with data, gave good advice and made the field tests possible.

Table of Contents

List of acronyms and abbreviations

ADC analog-to-digital converter.

APS Aerodynamic Particle Size.

CPC Condensation Particle Counter.

CSV comma-separated value.

GPIO general purpose input-output.

I^2C inter-integrated circuit.

IC integrated circuit.

MCU microcontroller unit.

MISO master in, slave out.

MOSFET metal–oxide semiconductor field-effect transistor.

NTC negative temperature coefficient.

OPC Optical Particle Counter.

PCB printed circuit board.

PETG polyethylene terephthalate glycol.

PM particulate matter.

PWM pulse width modulation.

RH relative humidity.

RPi Raspberry Pi.

RTC real-time clock.

SMPS Scanning Mobility Particle Sizer.

SPI serial peripheral interface.

TEOM Tapered Element Oscillating Microbalance.

TI Texas Instruments.

WHO World Health Organization.

1 Introduction

One can survive 3 weeks without food, 3 days without water and 3 minutes without air. Despite the importance of air to human lives, air quality is not something we typically reflect over in our everyday life. While we do react to smoke from fires or smog in big cities which are very high concentrations of air pollutants, we do not tend to react to low concentrations which we cannot see or feel. However, even low concentrations of air pollutants can have large health impacts. According to the World Health Organization (WHO) [31], 4.2 million deaths are annually attributed to outdoor air pollution and 3.8 million deaths are claimed to be the result of exposure to household air polluted by eg. smoke from cooking stoves. Deaths related to air pollution are mainly caused by lung cancer, chronic obstructive pulmonary disease (COPD), stroke, lower respiratory tract infection (LRTI) and heart disease. The four air pollutants that are considered to have the highest health and environmental impact are particulate matter (PM), ground-level ozone (O_3), nitrogen dioxide (NO_2) and sulfur dioxide (SO_2).

While some sources of air pollutants have natural causes like sand storms or forest fires and can't be avoided, a great part comes from burning of fossil fuels, industry, waste treatment and agriculture. Guidelines [32] and regulations [1] have been introduced to define limits and minimize these emissions. As an EU member state, Sweden is, for example, obliged to monitor and report the air quality. The main responsibility to measure air pollutants in Sweden lies with municipalities who run and control air quality measurement stations. Together these stations create a nationwide network which generates data that can be used as a foundation for taking suitable actions to reduce emissions. The instruments used are generally expensive and space consuming, and can only be used on selected locations.

Recent sensor technology development have made cheap and compact low-cost particulate matter sensors available. Low-cost particulate sensors can be purchased for as little as 300 SEK [30] (Nova PM sensor SDS011), thus allowing the deployment of multiple sensors at different locations. This could mean increased coverage and better data resolution as compared to the limited resolution from the measurement stations. Today, the measurement values from these sensors are however often sensitive to variables such as temperature and humidity [2]. High-end sensors do not generally suffer from these same sensitivities in the same way because of built-in measures to reduce this.

1.1 Problem statement

One of the most well-known factors that affect low-cost particulate matter (PM) sensors' reliability is the relative humidity [33][2][6][3]. Some particles are more hygroscopic than others and may change in size due to their absorption [40]. This increases the light scattering [26] of the aerosols. These combined effects will negatively affect the reading of an optical particle counter.

The main objective of this thesis is to build a prototype that can improve existing low-cost PM sensors, allowing them to deliver good results even in a humid environment. Hardware methods to reduce the relative humidity were investigated as part of the prototype development process. To evaluate the performance of the prototype a series of low-cost PM sensor tests were conducted both with and without the prototype.

1.2 Existing solutions

It is possible to theoretically compensate for humidity induced errors [8]. Assuming a known aerosol composition of the measured volume the theoretical dry diameter of particles can be calculated [40] and used instead in the calculation of mass concentration. The particulate matter (PM) mass concentration calculated this way should compensate for the hygroscopic growth of particles in wet conditions. Another way to compensate for error is to create an empirical model. This method requires that both reference data and sensor data is collected at the deployment location, or at a location where the particle composition is about the same. Based on that data a regression model can be created. Other ways to compensate such as machine learning algorithms have also been used in studies [5].

Additionally, there are a number existing methods and instruments to dry air physically. This includes membrane drying [34], diffusion [14] and heating [15]. These existing air conditioners are, however, quite expensive and large when compared to low-cost PM sensors.

1.3 Report outline

This report begins by introducing some basic aerosol terminology to the reader. It explains also how relative humidity affects the airborne particles and presents common methods used to measure the particulate matter. The method section presents the sensor used in the study, describes the steps taken to develop the prototype and how the evaluation of the sensor was realized. In the results section, the reader can find a visualization of the gathered data in multiple plots. The final part presents the outcome of the thesis and discusses possible improvements and future work.

2 Theory

2.1 Aerosols

An aerosol is defined in its simplest form as solid or liquid particles suspended in a gas. The term aerosol thus describes a two-phase system; the particles in the gas and the gas itself. Aerosols exist everywhere around us from a variety of sources; power plants, cars, soil, and salt particles formed from ocean spray. A naturally occurring aerosol is where condensation of water in the atmosphere may result in the formation of different shapes - a phenomenon known as clouds. Since it has been shown that excessive exposure of certain aerosols may lead to increased health risks a major part of aerosol science relates to how aerosols affect our health [12].

A common way of distinguishing between the type of particles is with their diameter (d_p). This is because a particle's size tells a lot about its properties [12]. Bigger particles typically fall to the ground quickly while smaller particles can stay airborne for a long time and for long distances. A recent example is when southern Sweden in the spring of 2019 measured huge spikes in particle concentration. The origin of these small sand particles was concluded to be from the Sahara Desert [41]. Smaller particles typically also penetrate the lung-blood barrier more easily and may possess increased health risks. A rough distinction is usually made between coarse particles ($d_p > 2\,\mu m$) and fine particles ($d_p < 2\,\mu m$). Another distinction commonly used when regulatory agencies set particle thresholds is PM1 ($d_p < 1\,\mu m$), PM2.5 ($d_p < 2.5\,\mu m$), and PM10 ($d_p < 10\,\mu m$) [27]. The range of particle size can vary greatly, from $0.001\,\mu m$ to over $100\,\mu m$ [12].

2.1.1 Humidity theory

Small particles may attract water molecules if the humidity is high enough [12]. This can result in particles changing in size and mass which creates a problem when trying to measure aerosols; how do you make sure that you get a reading that is independent of the humidity in the air? To get a grasp of humidity and how it influences particles, a few definitions will be elaborated below. These definitions will be assumed to be about water and its vapor but are valid for all substances.

Partial pressure (p) is the pressure that a gas in a mixture of gases would exert if it were the only gas in the entire volume occupied by the mixture. If there is only one gas, the partial pressure is the same as the total pressure. If there are several gases, the total pressure is the sum of all partial pressures in the mixture. For a certain atmospheric pressure in the atmosphere, the partial pressure of water vapor is correlated with the fraction of vapor that exists in the air. The partial pressure thus depends on the atmospheric pressure and the mass concentration of water vapor [12].

Saturation vapor pressure (p_s) is the partial pressure required to maintain mass equilibrium between vapor and its liquid or solid flat surface. It relates to how easy it is for water molecules to evaporate from the water surface. It can be said that when the same number of particles are evaporating as they are condensing on the water surface, equilibrium is reached. At that point, the partial pressure of the evaporated water vapor will be the same as the saturation vapor pressure at that temperature. The saturation vapor pressure depends on temperature and the type of substance [12].

$$RH = \frac{p}{p_s} \cdot 100$$

Relative humidity (RH) is the ratio between p and p_s expressed in percent. It tells how saturated the air is. If p is less than p_s, particles that evaporate will remain as vapor. This is called the undersaturation. If p is more than p_s, water that evaporates will instantly condensate again, and vapor in the air will tend to condense if possible. This is called oversaturation. Saturation ratio is another definition sometimes used and is directly translated as RH/100 [12].

An interesting aspect is how relative humidity can be modified. At least two parameters seem to be quite easily influenced; the vapor mass concentration and the temperature. Changing the vapor concentration seems quite intuitive; removing the vapor will result in a lower vapour partial pressure and the humidity will decrease, and vice versa. As also described, the saturation vapor pressure is dependent on temperature. An increase in the temperature will result in an increase in the saturation vapor pressure. This means in practice that the air will be able to hold more water vapor which then decreases the relative humidity. Lowering the temperature will decrease the saturation vapor pressure, which if the air gets oversaturated can result in water vapor starting to condensate.

2.1.2 Particle growth

It is possible for water to condensate without a nucleus, i.e. without something to grow on. This is called homogeneous nucleation. A quite high saturation ratio (> 3.5) is required for this to occur. A much more common way for water vapor to condensate in the atmosphere is by being attracted to small particles floating in the

air, called nucleated condensation. This is because a much lower saturation ratio is usually required to allow for condensation. When water vapor condensates on these particles, the relative humidity will fall so that enough oversaturation won't be reached as to form homogeneous enucleations. Homogeneous nucleation will thus not be further covered in this thesis due to its uncommon presence in normal atmospheric conditions [12].

2.1.3 Nucleated condensation on insoluble and soluble nuclei

Soluble nuclei here mean particles that are soluble in water. These have the property of being hygroscopic, meaning that they have the capacity to absorb water. As previously mentioned, oversaturation is usually required to allow for condensation. When no nucleus is available at all, the oversaturation needs to be quite high. When a nucleus is available to condensate on, an oversaturation of only a few percents usually is enough. A special case exists; when a nucleus is hygroscopic, condensation may occur even when the air is undersaturated, i.e. when the relative humidity is below 100%. It will here be explained for salts but is the same for all soluble compounds [12].

A common soluble particle in the atmosphere is NaCl, normal table salt. These form largely due to ocean spray that atomizes small salt particles in the air. As is well known, when salt is added to water the boiling points increases. It does so by rearranging the molecules so that the water and salt molecules interact, resulting in a lowering of the saturated vapor pressure above the water surface. This changes the balance between water that is evaporating and water that is condensing so that a reach of equilibrium will require an increase in temperature. This will compensate for the effect of the added salt so that the saturated partial pressure (which is dependent on both temperature and substance) again may decrease and allow for boiling to occur [12].

The process is the same when applied to nuclei instead of a pot of boiling water. Water that initially attracts the polar soluble molecules will have a change of saturated vapor pressure, which then makes it more difficult for water to evaporate from the nuclei surface. Water will continue to condensate on the nuclei until equilibrium is reached. This allows for growth by condensation to occur at a lower saturation ratio than for pure water (below 100% RH) [12].

Many salt particles have an additional hysteresis effect so that droplet formation occurs at a higher humidity level than the re-crystallization does. Due to this, many particles experience an "activation" of absorption when the humidity passes a certain level [12].

2.2 Measurement techniques

There are many ways to measure aerosols, each having their own advantages and disadvantages. Some are more exact but more expensive and space consuming. Some can measure the whole particle spectrum while some are limited in their range. Some instruments measure size primarily while some measure mass. Some instruments can determine the size distribution of particles while some cannot. There truly isn't any optimal instrument for every application.

The sensors being evaluated in this thesis are of the type Optical Particle Counter (OPC). The rest of the measuring techniques are used in reference instruments in the experiments of evaluation.

2.2.1 Optical Particle Counter (OPC)

Optical particle counting is a very sensitive way of counting and sizing particles and has a lot of advantages. The technology can be modified to be cost-effective and not take up much space. The aerosol is also minimally disturbed with this technique, reducing error sources in the measurement. The measurement is continuous and provides instant feedback. A final advantage is that it, unlike some other techniques, is possible to get a size distribution of the particles counted [12].

How optical particle counters work exactly differs between different manufacturers, but the basic constructions utilize a light scattering technique where laser light is being optically focused on a detection zone placed in a flow of an aerosol, see Figure 1. When a particle passes over the detection zone and laser beam, the laser light will scatter and change direction. The scattered light then gets focused on a photo-detector, where the intensity of the light can then be used to calculate the size of the particle among other things. Particles down to 0.1 µm can theoretically be measured with this type of technique, but most manufacturers put a limit around 0.3 µm on its instrument [12].

There are some error sources with Optical Particle Counters that are inherent to the design. Some of these errors are possible to limit in lab conditions while it may prove more difficult in atmospheric conditions where the environment is less controllable.

- Assumptions need to be made - A disadvantage with optical particle counters is that some assumptions need to be made to calculate properties of the particles. Among these assumptions are the refractive index and density of the particle. Refractive index is used to calculate the size of the particle from the scattering intensity, while the density is used to convert from size concentration to mass concentration which is a common unit used in

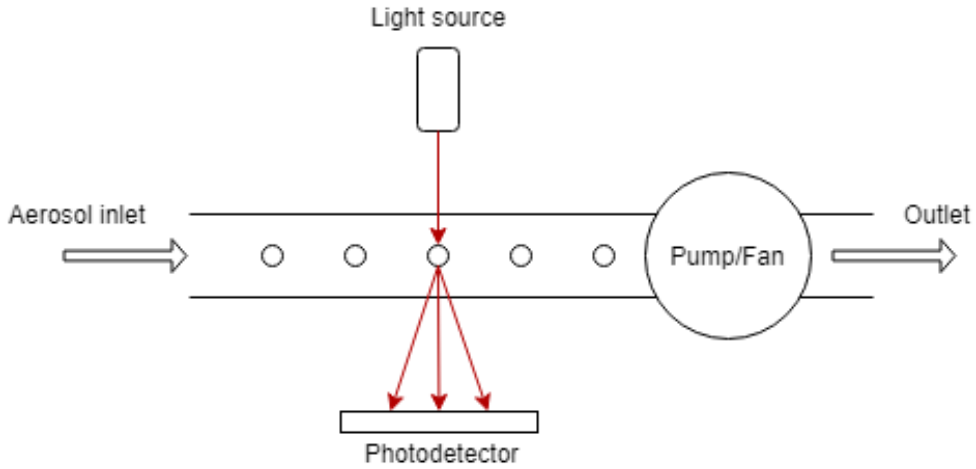

Figure 1: Working principle of an optical particle counter. Figure adopted from [12, Fig. 16.8]

aerosol measurements. Especially refractive index can vary greatly within a polydisperse aerosol (an aerosol with different kinds of particle sizes), and due to this the error in measured size can range from 30% to 400% [12].

- Coincidence error - Another type of error that may occur for high concentrations is when more than one particle is in the detection zone at the same time. Instead of being sensed as two separate particles, it can from the photodetector's perspective look like as if there is one big single particle. The result of errors due to coincidence will be an underestimation of the particle concentration and an overestimation of the particles' size. The maximum number of particles allowed to avoid more than 5% coincidence errors depends on the specification of the instrument, but a number concentration of less than $1000/cm^3$ is generally necessary [12].

- Doesn't cover whole range - The spectrum of particles in the atmosphere varies greatly, down to a few nanometers up to several micrometers. Due to the optical particle counters size limit, particles below the detection limit will not be counted. This may result in measurement errors when compared to other instruments that use technique that measures the full range of particles [12].

2.2.2 Aerodynamic Particle Size (APS)

The APS is an instrument developed by TSI Instruments which has a patented technology that uses the principle of inertia to determine the size of a particle. In the instrument, an aerosol gets accelerated when forced through a nozzle. Because

of differences in the properties of particles, such as mass and size, the acceleration of different particles will vary. Bigger particles typically accelerate slower while smaller accelerate quicker. Two laser beams are placed close to each other in the path of the moving aerosol. When a particle passes through a laser beam, light scatters and gets picked up by a photodetector, see Figure 2. The peak-to-peak time between the two laser beams can then be used to determine the aerodynamic size of the particle. The sizing range goes from 0.5 µm up to 20 µm [16].

The APS assumes density to calculate the size of the particle and is also sensitive to coincidence errors. This error is although limited the light scattering signal is used to determine if the measurement is faulty. For instance, if more than two peaks are detected within the detection threshold it is assumed to be due to coincidence, and the count is placed in a separate bin [16].

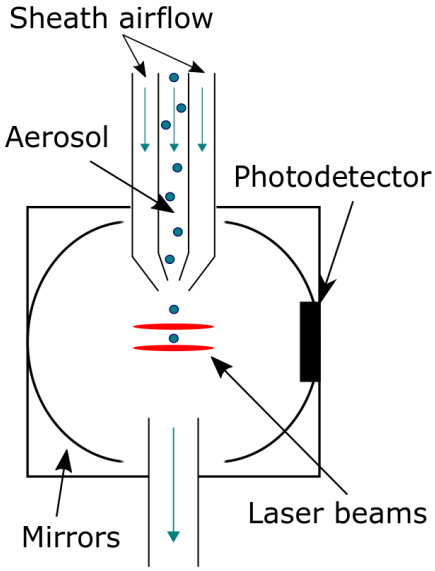

Figure 2: Working principle of an APS. Figure adopted from [4]

2.2.3 Scanning Mobility Particle Sizer (SMPS)

This measurement technique uses two stages. The first stage of the SMPS is to separate a single size of particles from a polydisperse aerosol. The second stage is for the Condensation Particle Counter (CPC) to count this now monodisperse aerosol (an aerosol with only one kind of particle size). By scanning through different sizes of particles with the SMPS and then counting them with the CPC, a particle distribution of the aerosol can be built up [18].

The separating in the SMPS works by utilizing that the electric mobility of a particle is inversely related to the size of the particle. Electric mobility means its ability to move through an electric field. By creating an electric field in the middle of a piston, the specific attraction to the piston depending on particle size makes it possible to extract the desired size of the particle, Figure 3 show the working principle of this separation method [18].

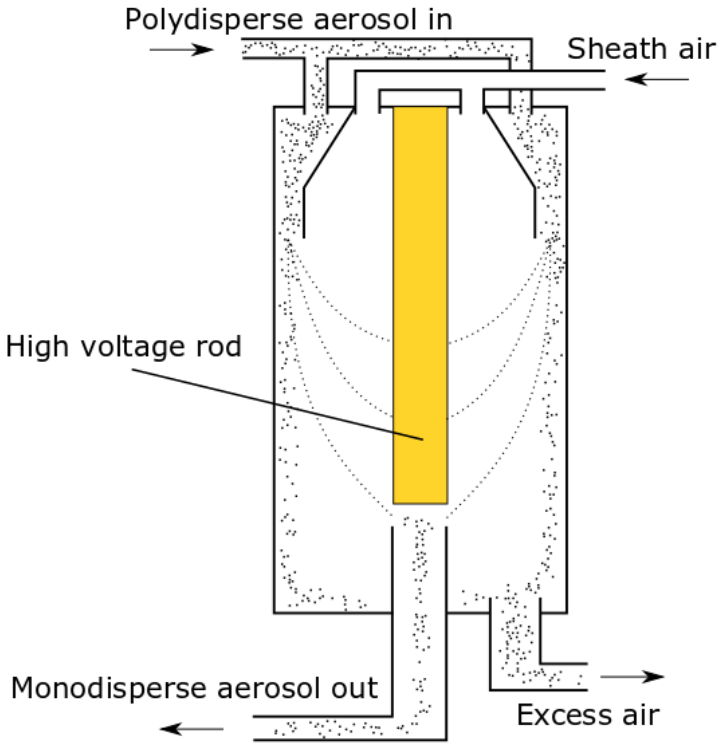

Figure 3: Working principle of particle separation in the SMPS.

Counting with the CPC is similar to the OPC. A laser is illuminating a detection area where the light scatters when a particle gets illuminated. The scattered light gets detected with a photodetector. One difference is although necessary since the SMPS can separate particles that are below the size threshold for normal optical counters. For these to be counted by the CPC utilizes condensation to make particles grow so that they're easier to count. This works by injecting butane vapor in the same chamber as the aerosol. The temperature after that gets decreased so that the butane condenses on the small particles, resulting in an increase of size. This droplet can then be counted by the CPC. Note that the CPC doesn't provide any size

measurements since this already has been done by the SMPS [17].

The measurements with this technique are very precise and do not assume density or optical properties of the particle, eliminating those error sources. The detection limit is down to 1 nm up to 1000 nm [18].

2.2.4 Tapered Element Oscillating Microbalance (TEOM)

The TEOM is a gravimetric measurement method, meaning that particle concentration is measured by determining the weight of particles. This works by having particles go through an inlet that isolates particles below a certain size, such as PM2.5. The aerosol then passes a filter where the particles get stuck. By oscillating the filter with magnets and then determining the response frequency of the filter, the mass on the filter can be calculated [37].

TEOM is commonly used as a reference instrument for monitoring government thresholds. Drying of the aerosol before being led through the filter is usually employed so as not to weigh the water. The size distribution cannot be determined with this method.

3 Method

A big part of the work in this thesis was about preparing tests and collecting data. The low-cost particulate matter sensors used for the measurements had to be enclosed to withstand weather conditions and interfaced in a way that allowed the collected data to be related to other sensors. Apart from the low-cost PM sensors many other instruments, sensors and components were used to collect needed reference data, gather the environmental variables or control the air conditioner. All of the above hardware as well, as the software, are described in the next two sections. As the main goal has been to evaluate a hardware way to reduce relative humidity (RH) induced errors a short study was made to find a suitable alternative to already existing solutions. This study follows some practices from the concept development framework presented by Ulrich and Eppinger[42].

Data used in the evaluation was gathered in two ways. The first way was to conduct 2-3 weeks long field test of the standard low-cost sensors and the additional long field test of after the low-cost sensors were equipped with the prototype. The second way was to test the low-cost sensors with and without the prototype in a controlled environment in the aerosol laboratory at LTH. The testing procedures are described in more detail in sections that follow.

3.1 Low-cost PM sensors

Alphasense OPC-N2

The main sensor used in this thesis was an Alphasense OPC-N2 shown in Figure 4. As the name indicates it is an optical particle counter sensor type. Sensor size is roughly 7.5cm x 6.4cm x 6cm, it has an inlet with 7mm diameter and four M3 mounting holes on the inlet side. On the opposite side, sensor is equipped with a 3cm x 3cm fan that creates the airflow through the sensor, see figure Figure 5. Sampled air enters through the inlet and continues to a chamber where a laser lights up the sample airflow. Scattered laser light that reflects from airborne particles is captured and its intensity measured. OPC-N2 can detect particles ranging from $0.38\mu m$ to $17\mu m$. It can classify and count particles in 16 different size categories called bins.

The mass concentrations of PM1, PM2.5 and PM10 are calculated by the sensor from the particle counts assuming a particle density of $1.65 g/ml$ and refractive index $1.5 + i0$ [24] for all types of particles.

Figure 4: Alphasense OPC-N2 has four mounting holes spread around the inlet that make it easy to mount the sensor in enclosures. The sensor is also equipped with Molex PicoBlade connector for the serial peripheral interface (SPI) communication and a micro USB connector for access to the built-in SD card.

The sensor can be either interfaced by SPI [7] or autonomously sample data and store it on the built-in 16GB SD card. Data stored on the SD card can be accessed after the measurements from a computer through a micro USB port. SPI port can be used to either connect to a PC through a USB-SPI adapter or to an SPI Master device, for example, a microcontroller unit (MCU). In the latter case, it is only possible to communicate one sensor at the time. When using the adapter official software can be used to record and watch data in real-time. Sensor requires 5V and 175mA while measuring which can be provided to it by the power pins of SPI port or by the micro USB cable. The cost of one unit as of December 2018 was 317 EUR. Complete sensor specifications are shown in Table 1.

Three OPC-N2 units were used in the thesis, named below:

1. One-year-old and the previously used unit, N2-1

Table 1: Specifications comparison of Alphasense OPC-N2 and OPC-N3[24, Tab. 1][25, Tab. 1]

Feature	*OPC-N2*	*OPC-N3*	*Unit*
Measurement			
Particle range Spherical equivalent size (based on RI of 1.5+i0)	0.38-17	0.35 to 40	μm
Size categorization (standard). Number of software bins	16	24	
Sampling interval. Histogram period (recommended)	1-10	1-30	s
Total Flow rate (typical)	1.2	5.5	l/min
Sample flow rate (typical)	220	210	ml/min
Max particle count rate	10000	10000	particles/s
Min detection limit (PM10)	0.01	0.01	$\mu g/m^3$
Max detection limit (PM10)	1500	1500	$\mu g/m^3$
Coincidence probability	0.84	0.8	% at 10^6 particles/l
Power			
Measurement mode(typical)	175	180	mA
Non-measurement mode(typical). Laser at minimum power; fan off	95	45	mA
Transient power on start-up	<5000	<5000	mW for 1ms
Voltage range	4.8 - 5.2	4.8 - 5.2	V DC
Key specifications			
Digital Interface	SPI(Mode 1), USB 2.0	SPI(Mode 1)	
Data storage(micro SD)	16	-	GB
Laser classification(enclosed housing)	Class 1	Class 1	
Temperature range	-20 to 50	-20 to 50	°C
Humidity range(non-condensing)	0-95	0-95	%RH
Weight	<105	<105	g

Figure 5: Small fan on the OPC-N2 that creates the airflow through the sensor.

2. The brand new unit, N2-2
3. The brand new unit, N2-3

Alphasense OPC-N3

OPC-N3 is the successor of OPC-N2. The physical shape and working principle are the same as of the older model however the specifications have changed. OPC-N3 can detect particles in the range from $0.35\mu m$ to $40\mu m$ and classifies them in 24 bins. Maximum airflow was increased to $5.5l/min$ and the sensor was equipped with a combined temperature and humidity sensor SHT31 located on the printed circuit board (PCB). OPC-N3 has also modified the airflow path to reduce turbulence and particle deposition in environments with high particle concentration. Figure 6 show an OPC-N2 beside an OPC-N3.

Five OPC-N3 units were used in the thesis, named below:

1. The brand new unit, N3-1
2. The brand new unit, N3-2
3. The previously used unit, N3-3
4. The previously used unit, N3-4
5. The brand new unit, N3-5

Complete specifications of the OPC-N3 are presented in Table 1

Figure 6: Alphasense OPC-N2 on the left and Alphasense OPC-N3 on the right. From the outside, they look identical.

3.2 Study of hardware methods to lower RH

A study of different methods to lower the relative humidity has been made in order to find the most suitable one. Techniques from product development framework by Ulrich and Eppinger [42] were used in this study to clarify the limitations and facilitate the choice of a suitable solution.

Similarly as in [42, Fig. 6.2] the features of the hardware method are presented in Table 2. These features reflect the main functionality of the desired solution e.g. the fact that the prototype should match the compact size of a low-cost PM sensor.

To further specify the requirements of the air conditioner a list of the desired and measurable properties was created. The properties and desired values originate from the features but also the sensor manufacturer's recommendations [24] as well as the literature [22, Ch.6.3]. All the properties are presented in Table 5 in Appendix B.

3.2.1 Concept generation

Concepts were generated continuously as the ideas came up during the reading of the literature, looking at sensor data and while researching for existing solutions.

Table 2: Features that the hardware prototype should provide. Similar as in[42, Fig. 6.2]

Index	***Needs***	***Weight***
	Function	
1	Improves OPC's accuracy in high RH	5
2	Works independently of particle disposition	3
3	Little particle loss	4
4	Does not disturb sensor function/ complies with sensor specification	5
	Form	
5	Has high energy efficiency	2
6	Has a compact size	3
7	Low cost	4
8	Low complexity	3
	Safety/maintenance	
9	Is safe to deploy unsupervised	5
10	Requires little to no maintenance	4
	Installation	
11	Easy to install	4

Apart from that, a brainstorming session was held with engineers not involved in the project. This session resulted in additional ideas on how to lower the relative humidity of the air. All the hardware concepts are briefly presented below.

Outer heating A pipe is attached to the sensors and heated with electric heating pads or cables. The pipe conducts the heat and warms up the air flowing through it. The outside of the pipe and the heating element is thermally isolated to direct the heat inwards thus minimizing energy loss. See Figure 7.

Inner heating A pipe is attached to the sensor with a resistive heater in the middle of the pipe. The heater will heat the air directly and as a consequence lower the RH. This concept should have higher efficiency since the air is heated directly by the heater and not like in the outer heating concept through the pipe. However, it's hard to place the heater inside a pipe without affecting the airflow. See Figure 8.

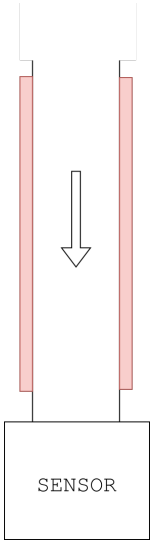

Figure 7: Outer heating concept

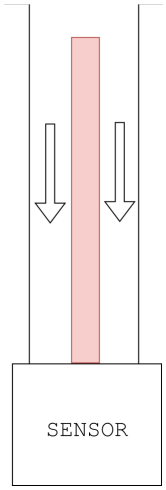

Figure 8: Inner heating concept

Induction heating A variation of outer heating concept shown in Figure 7. The pipe is heated by induction heating instead, thus warming the air inside the pipe and lowering the RH. See Figure 9.

Straw heating The inlet air is split up into smaller channels, "straws", which are conducting heat coming from a heat source. This design maximizes the heating surface which air is exposed to. See Figure 10.

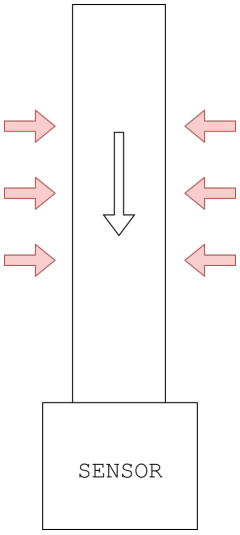

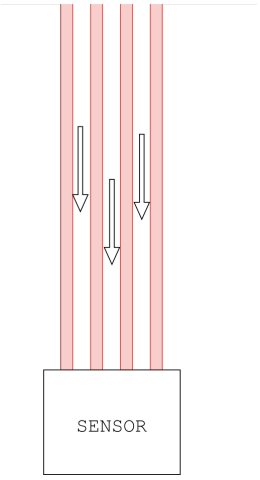

Figure 9: Induction heating concept

Figure 10: Straw heating concept

Condensation drying

A Peltier module is attached on an inner pipe with the cooling part directed outwards and heating part inwards. Entering air will first be cooled to reach the water saturation level. Water will then condense on the cold surface of the Peltier module. The absolute humidity of the air will be reduced at that point. The cold air can then be heated by the hot side of the Peltier module inside the pipe. Heating the cold air with less water content will result in lower RH of the air coming into the sensor. See Figure 11.

It is, however, questionable whether the condensed water would trap particles that could otherwise get measured.

Dilution drying Filtered and dry air is mixed with the sampled air. This lowers the absolute and relative humidity of the sampled air. The aerosol concentration is also lowered which must be adjusted in the results. See Figure 12

This concept requires that filtered and dry diluting air source is available. This can be achieved with either with a filter and an arbitrary drying method or a supply of clean and dry air.

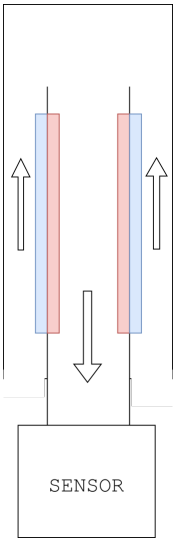

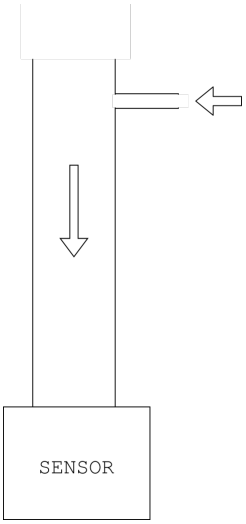

Figure 11: Condensation drying concept **Figure 12: Dilution concept**

Diffusion drying The inlet air is passing through a channel with walls made of an absorbent such as silica. Silica is highly hygroscopic and will absorb the moisture from the inlet air, thus reducing the absolute and relative humidity. See Figure 13.

The absorbent will eventually become saturated with water and will then stop absorb more. When that happens the absorbent could be replaced by a fresh one. In the case of silica, it is possible to dry it by heating it up to 110 degrees. This process could be automated to maximize uptime and minimize maintenance.

Membrane drying The inlet air passes through a hose made of a membrane, such as Gore-Tex, surrounded by a negative pressure differential air on the other side of the membrane. This will make water molecules want to move from the inlet air through the membrane to the surrounding air. Thus the absolute and relative humidity of the air the passing along membrane will be decreased. See Figure 14.

A disadvantage is that the pump is needed to produce the negative pressure in the air surrounding the membrane.

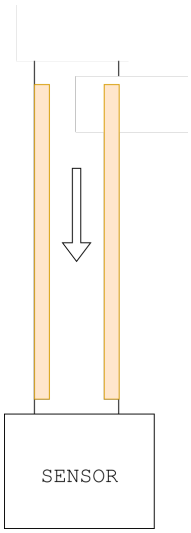

Figure 13: Diffusion drying concept

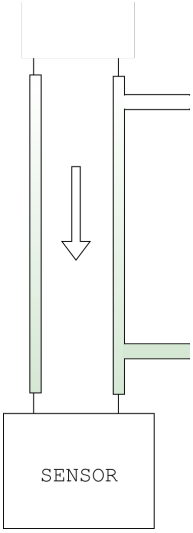

Figure 14: Membrane drying concept

3.2.2 Concept choice

Concepts were grouped based on the way they lower the relative humidity. Heating was chosen as the reference method because it is the most straightforward and the easiest method with which to change the relative humidity. A scoring matrix as in [42, Fig. 8.7] was used to grade these methods against the reference based on several criteria. The criteria used in the matrix were derived from the features presented in Table 2 and are explained below.

Table 3 presents the outcome of the first concept screening.

1. ***Requires no maintenance*** Prototype should be maintenance free to match the low-cost sensor which is claimed to be maintenance free by the manufacturer.
2. ***Independent of aerosol composition*** The physical prototype should be universal and work despite the location and variations in the aerosol composition.
3. ***No particle loss*** To give accurate measurements the prototype shouldn't negatively affect the air composition. Two aspects are taken into account by these criteria.
    - The inlet should be constructed in such a way that the flow through the inlet is laminar and particles do not get attached to walls.
    - The inlet should be made of electrically conductive material to minimize the effects of static electricity [22, Ch. 6.3].

4. ***Low cost*** The cost of the prototype shouldn't exceed the cost of the sensor.

5. ***Energy efficient*** The prototype should be energy efficient relative to the low-cost sensor power consumption and it should preferably run on low voltage.

6. ***Compact size*** Low-cost Optical Particle Counter (OPC) sensors are small size and thus can be used as a component in other products. The prototype should be also compact size to fit into those products.

7. ***Complexity*** The prototype construction should be simple, for increased robustness, shorter development and lower cost.

Table 3: Screening matrix for different concepts that can lower the relative humidity. Air heating is a reference and score range is 1 to 5, where 1 is worst and 5 best score. Matrix is similar as in [42, Fig. 8.7]

		Concept				
Criteria	***Weight***	***Heating (Reference)***	***Dilution***	***Diffusion***	***Condensation***	***Membrane***
Requires no maintenance	20%	**3**	1	2	3	2
Independent of aerosol composition	15%	**3**	3	3	3	3
No particle loss	15%	**3**	4	3	2	3
Low cost	15%	**3**	1	2	3	1
Energy efficient	8%	**3**	1	4	3	2
Compact size	15%	**3**	1	2	3	1
Complexity	12%	**3**	1	2	3	1
Weighted score		3	1,75	2,46	2,85	1,88

Motivation for criteria scores:

Requires no maintenance

The dilution method requires a particle free and dry air supply which can be achieved with filters and an arbitrary drying method. These filters and additional drying methods raise the need for overall maintenance. The

diffusion method also requires a water adsorbent which eventually will be saturated at which time it must either be replaced or dried. The condensation method should be as maintenance free as the heating. The membrane itself does not necessarily need maintenance; however, the pump creating the flow around the membrane does.

Independent of aerosol composition

All physical methods are independent of aerosol composition. They should not need to be calibrated as is the case with the theoretical models.

No particle loss

The particle loss should be minimal in case of dilution. It is possible that the condensation method can capture some particles in the condensed water droplets.

Low cost

Dilution requires another drying equipment, filter and mixing chamber. The cost of the diffusion is mainly related to adsorbent cost and heater for the silica. The cost of the Peltier module is usually higher than the cost of resistive heaters. A Gore Tex membrane along with a pump is also a more expensive solution.

Energy efficient

Due to the fact that dilution method requires an additional dryer the energy efficiency of this solution is lower than that of the reference. Silica gel doesn't consume any energy; however, drying it up by heating does. If drying of silica gel doesn't have to be done so often it is a more efficient solution than just drying the air. The Peltier module is close to or little less energy efficient for heating than just a resistive wire.

Compact size

Dilution needs a separate dryer and mixing chamber. The diffusion prototype could be similar in size to the pure heating solution. It depends, however, on the airflow and amount of adsorbent needed to capture enough water. The Peltier modules are in the shape of small plates. A prototype with a Peltier module could be the same size as a resistive heater. The membrane dryers have acceptable size and shape; however, the prototype needs a pump.

Complexity

Dilution is a complex solution, it requires preparation of dry, clean air and mixing it in controlled proportions to be able to correct the mass concentration. The diffusion method would require an additional heater and sensors to control the silica gel's adsorption properties and resetting process. Design of the

condensation prototype would be slightly more complicated than the heating. The membrane drying requires a pump and hoses.

According to the chosen criteria, heating is the most suitable method to apply on low-cost PM sensors. Several concepts based on heating were developed but the simplest, outer heating, was chosen for further empirical testing.

3.3 Heater development

3.3.1 Initial prototype

The first physical prototype was constructed from a 15cm long aluminum pipe with an inner diameter of 8mm and 1mm wall thickness. This diameter of pipe matched the outer diameter of the OPC-N2 sensor's inlet. As a heat source, a 12V and 11W heating cable was used. The cable is built from resistive wire wound around a non-conductive core and covered in silicone isolation. Heating cable was folded in half, wound around the pipe and held in place by a steel wire. Figure 15 illustrates how the heating cable is mounted on the aluminum pipe.

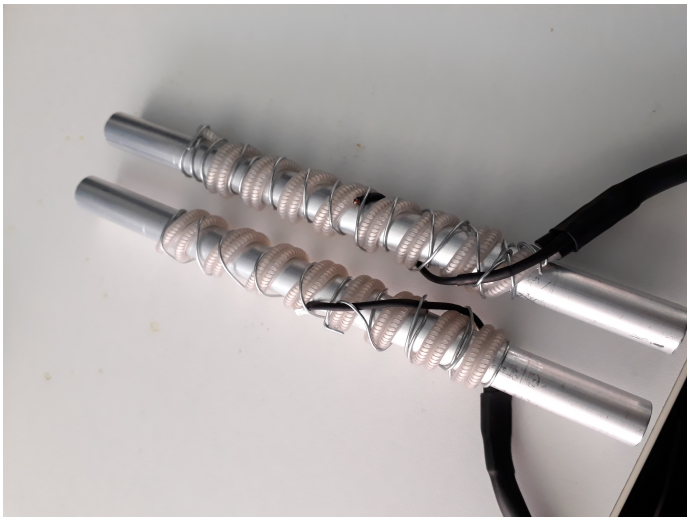

Figure 15: Heating cable wound around an aluminum pipe. The heating cable is held in place by steel wire. A small thermistor is placed on the heating cable and pipe with thermal paste.

Small negative temperature coefficient (NTC) thermistor was placed on the junction

of heating cable and pipe to read the temperature of the pipe. Air gaps around the temperature sensor were filled with thermal paste.

At this stage, a quick test was done to check the temperature of the pipe. The heating cable was plugged into a 12V power supply and run at maximum effect. The temperature was measured by converting NTC thermistor resistance into temperature with ATmega328p based development board. The temperature was plotted in real-time in a graph. The uncovered pipe as shown in Figure 15 reached $90°C$ in steady state.

Figure 16: Heating pipe isolated with 1 cm thick polyurethane foam.

The pipe was then wrapped with 1 cm thick polyurethane foam and once again the max temperature was measured. The insulated pipe, Figure 16 reached the temperature of around $125°C$. The next step was to verify how well the pipe can heat the air passing through it. The insulated pipe was attached to the OPC-N3 sensor with a short Tygon hose. In that hose, another NTC thermistor was fixed just by the inlet to OPC-N3. When running at the maximum effect the temperature of the inlet air was recorded to above $75°C$ while the temperature shown by the built-in sensor the OPC-N3 remained unchanged at $30°C$.

Before further tests the OPC-N3 was wrapped with a heating cable, equipped with a thermistor and isolated to minimize the suspected heat losses. A fourth thermistor

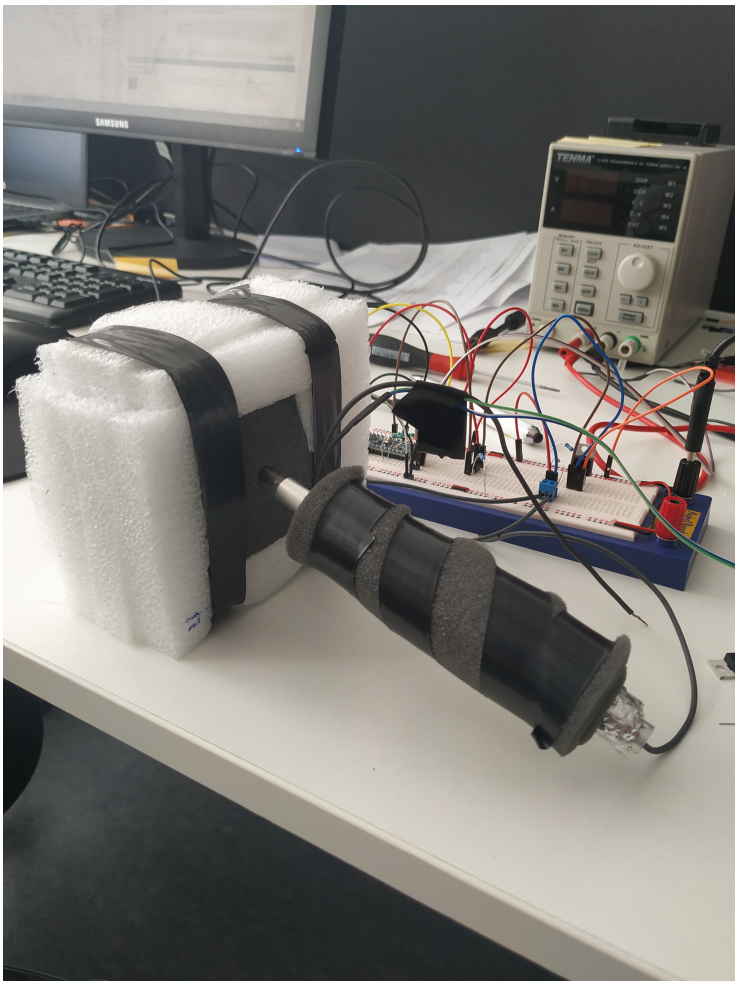

Figure 17: The initial prototype that was tested in the climate chamber.

was placed at the OPC's fan outlet. Figure 17 shows the isolated and heated OPC-N3 with a heated and isolated pipe attached to it. This prototype was placed in a climate chamber CTS C-40/350 [10] which can control temperature and humidity separately, see Figure 18. The performance of the heater was evaluated by testing the following worst-case scenarios:

1. The specified minimum operating temperature of the sensor is -10 degrees. The maximum operating temperature is 50 degrees. Thus, case one was to try to heat from -10 up to 45 degrees. Heating from the coldest possible temperature will have maximal heat dissipation due to the temperature difference. Purpose of this case was to test the maximum possible temperature increase.

2. One common and real case is low temperature and high humidity, typically seen in winters or early mornings. The maximum increase of temperature required to reach 30% is when the temperature is 6 degrees and maximum humidity, requiring a temperature increase of 26.3 degrees for a target temperature of 32 degrees [29]. Purpose of this case was to test if the goal in a realistic worst-case scenario is possible to archive.

3. Case 3 follows from case 2 by continuing to increase the temperature to 45 degrees if the goal for case 2 is reached. The purpose was to collect additional data.

4. For summer months, the temperature is usually higher, but humidity is lower. A worst case on a Swedish hot summer can be assumed 35 degrees and 60% RH. To reach 30% RH, the temperature needs increasing to 48 degrees [29]. This is an increase of 13 degrees. Purpose: If the previous test cases are reached then this target temperature should be reached as well. This is to be validated for this case.

Table 4 presents the results of heater performance tests. It can be seen that the desired inlet temperature and RH could be reached in all cases except the first one. Moreover, the OPC-N3 humidity sensor's readings were consistent with the target RH. This test results proved that the heater fulfills its main function which was to reduce the RH by heating the air. It was also observed that OPC-N3's built-in temperature and humidity sensor has a long reaction time, up to 30 minutes, which makes it ineffective for any control purposes. The heating and isolation of the sensor have also proved necessary in order to stop the energy loss and should be considered a new requirement for the final version of the prototype.

Figure 18: Initial prototype during the climate tests. Sensor wrapped in white isolation(on the left) with the heating pipe(on the right) which supported by a white block to keep the airflow line horizontal.

Table 4: Results of the climate chamber test of the initial prototype. Values are recorded from three sources: the climate chamber settings(Ext Temp and RH), thermistors placed on the prototype and the OPC-N3 internal sensor.

	Ext Temp [°C]*	Ext RH [%RH]*	Target	Inlet temp [°C]	Outlet temp [°C]	Pipe temp [°C]	Case temp [°C]	N3 RH [%RH]	N3 Temp [°C]**
Case 1	-10	n/a (70)	45	34	0	88	45	7.5	22.5 ->
Case 2	6 (9)	95 (92)	32	32	13.5	62	32	32	25 ->
Case 3	6 (8)	95 (93)	45	45	15	88	45	24.4	30.3 ->
Case 4	35	60 (52)	48	48	39	63	48	28.7	47.2

* Values within parenthesis are the actual values measured in the climate chamber.
** Values with an arrow mean that the temperature still was increasing at point of measure.

3.3.2 Final prototype

After proving the feasibility of the pipe based heater a more permanent version could be developed. One of the concerns was the material choice for pipe isolation. In worst case the heating cable could heat the pipe up to 120 °C which is too hot for most of the commonly available plastic foams. As an alternative, a cork block was used to isolate the heated pipe, see Figure 19. Cork has good thermal insulating properties [38] and was unaffected by the heat coming from the heating cable at its maximum effect.

Figure 19: Final isolation cut out from a block of cork.

A hole was drilled in the cork block to fit the pipe inside. Two parts were constructed to hold the pipe with cork together and to seal the ends. The first part shown in Figure 20 was designed to be attached to OPC's threaded holes. The middle hole was dimensioned to tightly fit the pipe and the conical collar to fit into the cork block. The notch in the collar fits cables to heating cable and thermistor while the walls around the part give extra support to the cork block.

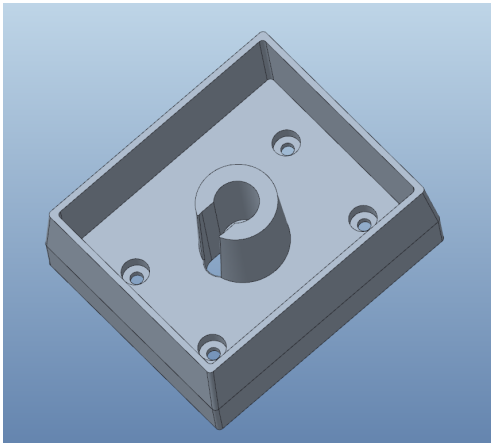

Figure 20: CAD model of the bottom plate which holds the heating pipe and isolation attached to the enclosure.

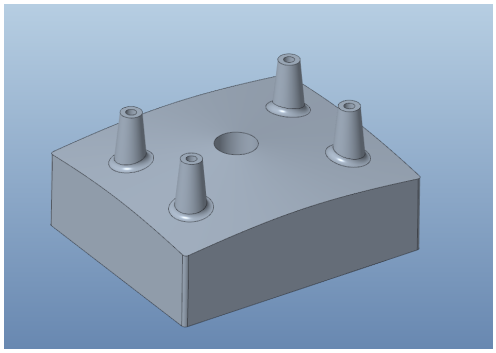

Figure 21: CAD model of the top end of the heater which holds the weather hat.

The bottom side of the second part (the side facing the cork) was designed similarly to the first mounting plate. The top side featured a curved surface to lead the water away from the pipe and mounts for the round pole cap which protected the inlet. The second plate is shown in Figure 21. Figure 22 shows the plates, the pipe and the cork block compared to each other. Both parts were 3D printed in polyethylene terephthalate glycol (PETG) plastic and their fit was tested before assembly. Final heater design attached to the enclosure is shown in Figure 23.

3.4 Field tests

The purpose of field tests was to evaluate the developed prototype's performance in ambient air where aerosol composition and concentration best represent one of the possible use cases for low-cost PM sensors. Dalaplan in Malmö, which is a highly trafficked urban area, was chosen as the test location. This choice was mainly based on the availability of PM instrument that can provide trustworthy reference data.

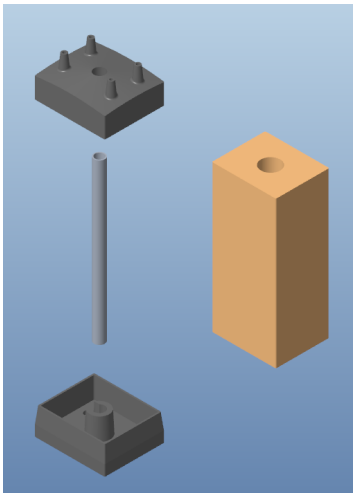

Figure 22: Exploded view of the simplified CAD model of the heater.

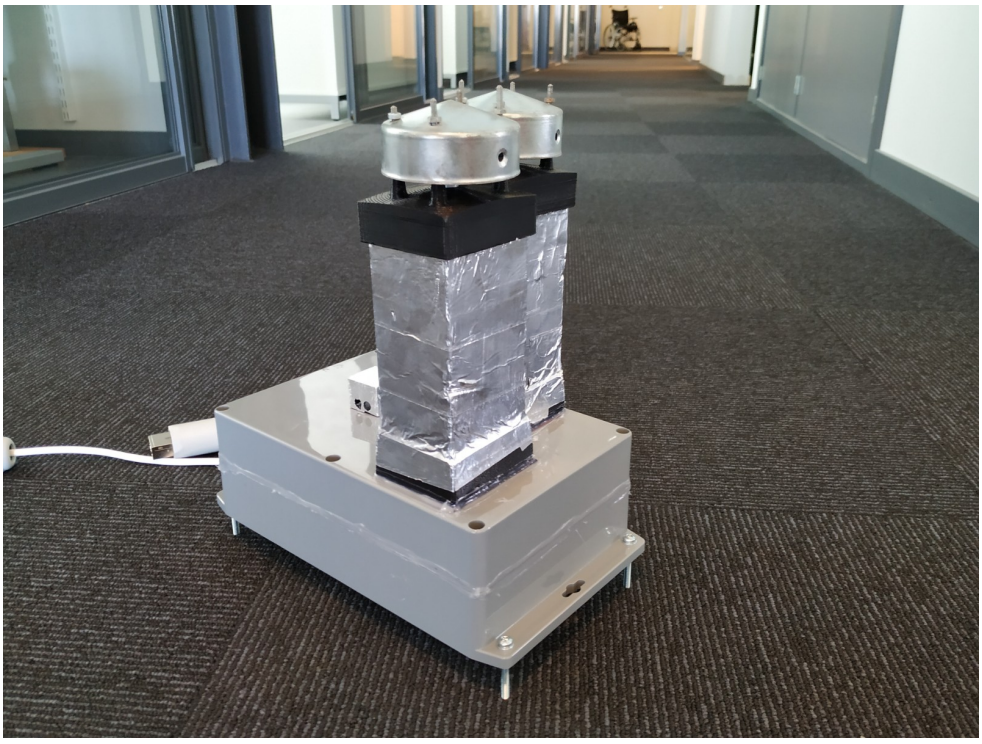

Figure 23: The final prototype mounted on the enclosure.

The instruments used as reference are placed in a permanent air quality measurement station, owned and maintained by Malmö Stad. The particulate matter measurements

Figure 24: Inlets of the air measurement station in Dalaplan. Mushroom shaped inlets are the cyclonic separators for PM sampling.

in the station are taken using the gravimetric method with two sets of TEOM 1400AB[36] combined with 8500 FDMS[35] conditioning system[23]. Air sampled by both sets enters through cyclonic inlets at a 3m height above the ground, see Figure 24. The cyclonic inlets allow only a certain size of particles to pass through. Hence two sets of TEOMs are used, one for PM 2.5 measurement and the other for PM 10, see Figure 25. Both TEOMs takes measurements in real-time and hourly data is available online[28]. For the purpose of this thesis, a minute data was kindly provided by Malmö Stad.

3.4.1 First field test

The first outdoor test was conducted at the early stage of the thesis project to gather data from unmodified sensors for later comparison. Before deploying the sensor a number of issues had to be addressed.

- The OPC-N2 sensors are delivered as OEM [24] version which means they are meant to be placed in another product or enclosed in additional housing to keep it weatherproof.

Figure 25: Field test reference instrument TEOM 1400AB with 8500 FDMS located in Dalaplan, Malmö. Unit on the left measures PM 2.5 and unit on the right PM 10.

- The OPC-N2 sensors can be provided with power and autonomously record data on the built-in SD card. The data saved in that way doesn't have timestamps since the sensor is not equipped with a real-time clock (RTC).
- The OPC-N2 cannot operate on a shared SPI bus i.e. one OPC-N2 requires one SPI port and cannot share it with other devices.
- Alphasense recommends that the OPC-N2 inlet is placed pointing upwards to reduce wind direction effect on sampling.
- The pole of the measurement station in Dalaplan had limited space for extra equipment.
- Temperature and relative humidity are not measured at Dalaplan.

A waterproof enclosure of suitable size was found and equipped with holes to fit two OPC-N2 sensors. Sensors N2-1 and N2-2 were attached in a row on the top half of the enclosure with threaded rods. To protect the sensor inlet from wind and rain, metal pole caps where attached to the threaded rods. This allowed adjustment of the height of the cap and the resulting air gap, see Figure 26.

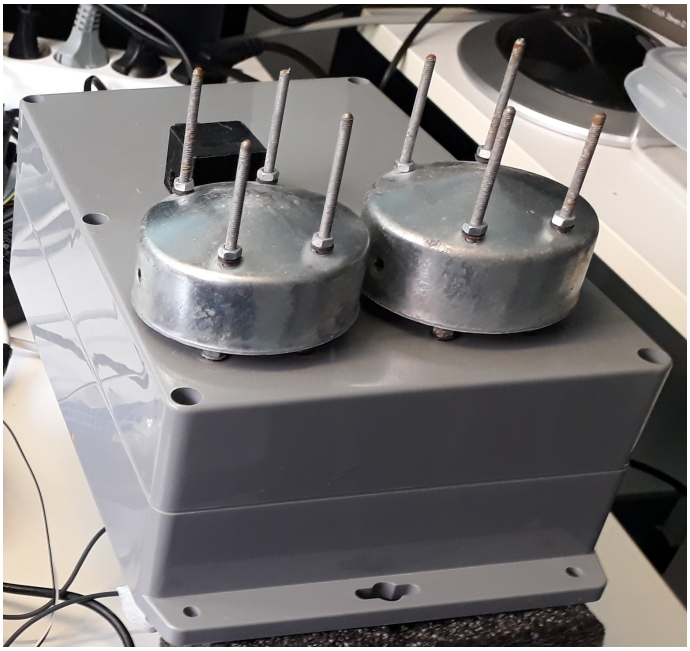

Figure 26: Measurement box used in the first field test. The pole caps protect the OPC-N2 inlets form wind and rain but leave a gap for the sample air. The small black box behind the pole caps is the protective case for temperature and humidity sensor.

Timestamps were the desired information which is especially useful when combining readings from different sources. The lack of that functionality in OPC-N2 sensors could be solved by communicating with them over available SPI port and saving retrieved data with timestamp by another device. A Raspberry Pi 3 B+ was used for that and a number of other reasons.

The Raspberry Pi (RPi) board is equipped with SPI and inter-integrated circuit (I^2C) interfaces to connect to sensors. It has Ethernet port allowing network connection and remote access to data. Once connected to the internet, the RPi can most importantly keep track of time. In addition, an already existing Python library for OPC-N2 [11] could be used on RPi to communicate with the OPCs. The limitation of one SPI per OPC sensor and the physical connections were solved by a custom designed board which is presented closer in subsection C.1.

Using RPi allowed to connect a temperature and RH sensor. SparkFun breakout board with Si7021 sensor chip, see subsection C.4, was chosen because of high accuracy, humidity working range of 0-100%RH, small size and ease of use. Ventilated case was also 3D printed for the sensor to protect it from the weather conditions.

An overview of all the components and how they are interconnected is presented in Figure 27.

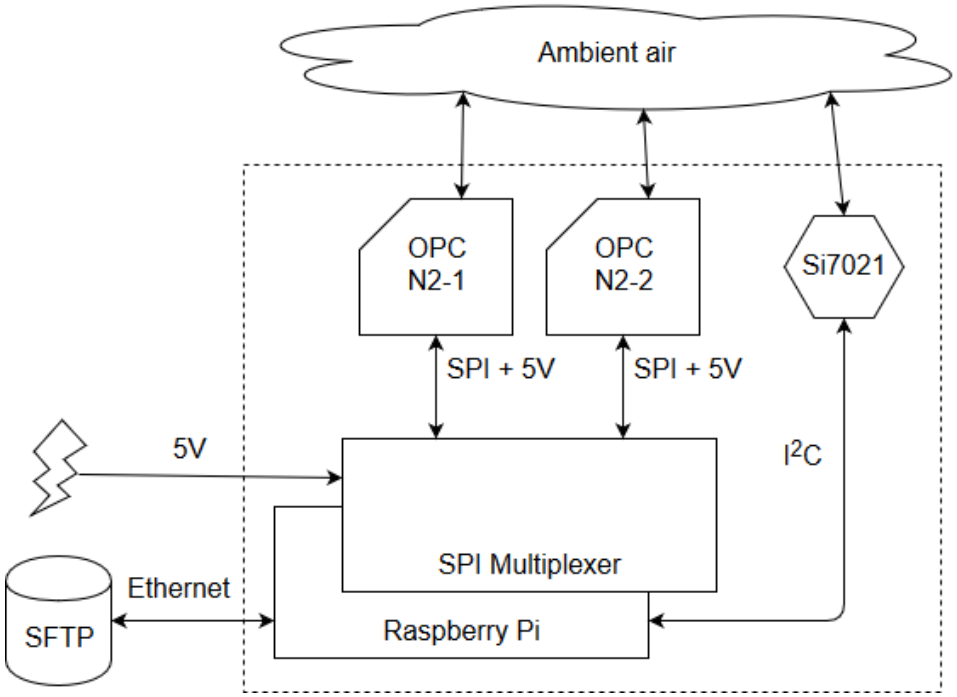

Figure 27: Schematics of the box used in the first field test.

The measurement box was placed in Dalaplan from 8th of February until the 1st of March. During that period the measurements were taken every 9 seconds which is just below the longest specified sample time. Python code was written to switch between the OPC sensors, read data, add timestamp, temperature, humidity and save data in comma-separated value (CSV) files. The files were frequently synchronized from the RPi to an SFTP server for easy remote access and as a backup in the case measurement box would be damaged.

3.4.2 Second field test

The second field test was the final performance test of the heated inlet prototype. This test was run from the 17th of April until the 5th of May. The box used in the first field was proved to be working well but for the second test it required few changes:

- Tests done during the heater development indicated that the OPC sensors should be heated and isolated to keep the desired RH within the sensor. For

those reasons sensors were aligned differently to allow a layer of isolating material between them and the enclosure walls.

- To provide enough power to the heating cables the voltage supplied to the box was raised to 24V and then stepped down with two DC-DC converters to 12V for the heating cables and 5V for the remaining components.
- New board featuring an MCU was built to connect and control heating cables as well as read temperature from the NTC thermistors, see subsection C.2 for more details.
- MCUs used in the new board was also equipped with an SPI port, the SPI board was no longer needed and was replaced by two identical boards of the new design, one for each OPC. Both new boards were communicating directly with the OPC and forwarded the information to the RPi through a serial port.

An overview of components and connections after the above changes can be seen in Figure 28. With the OPC sensors no longer directly connected to RPi the *py-opc* [11] could no longer be used and custom code was written to enable information exchange through the MCU.

During the climate chamber tests a temperature sensor was placed at the OPC's inlet, this sensor was removed in the final assembly to eliminate disturbance in the sampled airflow. The sensor was replaced by an empirical model describing the relation between the heated pipe and inlet temperature at different ambient temperatures. The model was created with data collected during climate chambers tests of the final heater prototype. Following equation was derived from that model

$$\begin{aligned} T_{pipe} = &-30.5936 + 4.4413 \cdot T_{inl} - 0.0633 \cdot T_{inl}^2 + 5 \cdot 10^{-4} \cdot T_{inl}^3 \\ &- 2.1682 \cdot T_{amb} + 0.0112 \cdot T_{inl} \cdot T_{amb} - 10^{-4} \cdot T_{inl}^2 \cdot T_{amb} \\ &+ 0.1189 \cdot T_{amb}^2 + 10^{-4} \cdot T_{inl} \cdot T_{amb}^2 - 0.0029 \cdot T_{amb}^3 \end{aligned}$$

where T_{pipe} is pipe's temperature, T_{amb} is ambient air temperature and T_{inl} is desired temperature at the sensor inlet.

The desired inlet temperature was calculated with the help of equations for saturated vapour density [29], shown below.

$$VD_{amb} = 6.335 + 0.6718 \cdot T_{amb} - 2.0887 \cdot 10^{-2} \cdot T_{amb}^2 + 7.3095 \cdot 10^{-4} \cdot T_{amb}^3$$

$$VD_{inl} = RH_{amb} \cdot VD_{amb} / RH_{inl}$$

$$VD_{inl} = 6.335 + 0.6718 \cdot T_{inl} - 2.0887 \cdot 10^{-2} \cdot T_{inl}^2 + 7.3095 * 10^{-4} \cdot T_{inl}^3$$

These equations combined along with the sensor readings were used to calculate the necessary pipe temperature for the targeted relative humidity in the sampled air.

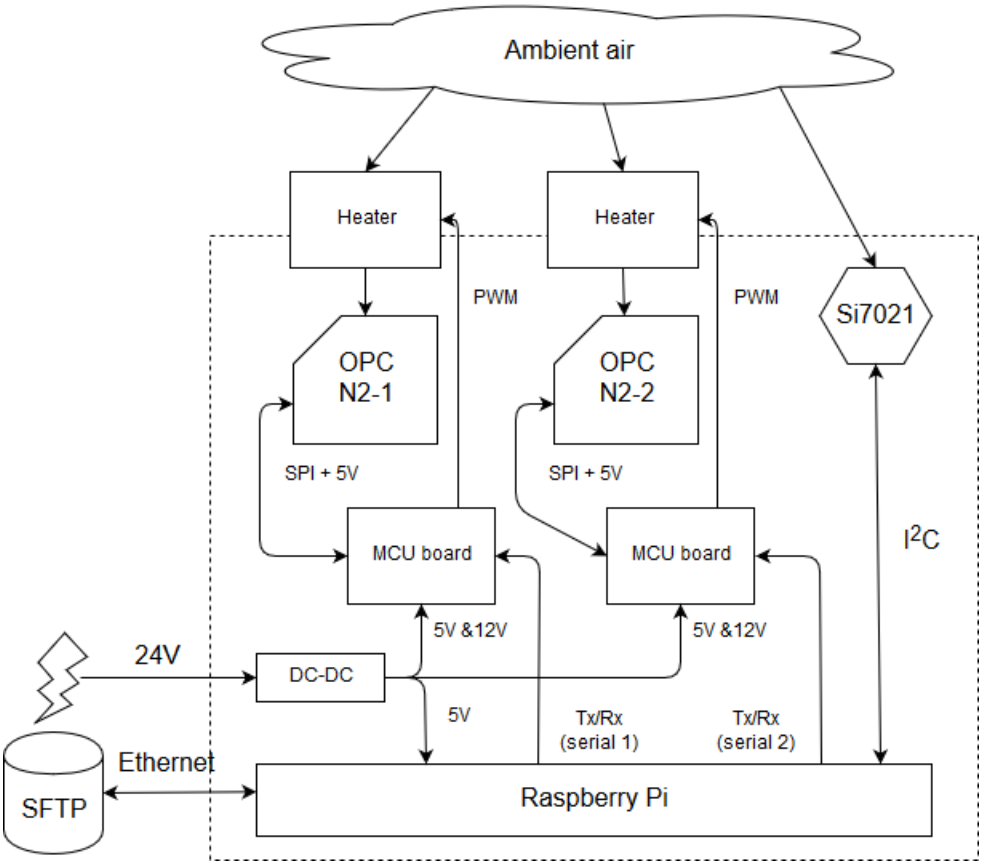

Figure 28: Schematics of the box used in the second field test.

The pipe temperature was calculated in the RPi and sent to the customized MCU board (subsection C.2) which in turn controlled the heater. The model could be also overridden by manually setting the pipe temperature or completely turning off heaters. This and more functionality was possible to set through a configuration stored on the SFTP server. The default settings of target 35%RH were used throughout the whole period of the second field test.

Figure 29a and Figure 29b show the outside and inside of the final prototype assembly used in the second field test.

(a) Outside, the two towers are heaters with inlet at the top.

(b) Inside, two OPC's are surrounded by foam isolation.

Figure 29: The complete measurement box that was used in the second field test.

3.5 Laboratory tests

3.5.1 Purpose

This experiment is a general-purpose test meant to get an idea of how a set of N2 and N3 sensors behave when exposed to a known hygroscopic particle with different ambient humidity levels. Due to a few size constrictions, up to 8 sensors can be tested at the same time to the same aerosol, thus enabling comparison between measurements. A combination of an APS (Aerodynamic Particle Sizer) and an SMPS (Scanning Mobility Particle Sizer) are used as reference instruments to get a measuring range containing the whole particle composition. Additionally, the heating prototype will be added to see if results improve in humid conditions.

3.5.2 Chamber description

A plastic box (79.5 x 58 x 44 cm) was divided into one mixing chamber and one sampling zone. The two chambers were divided by a perforated sheet with 466 evenly distributed holes. Sensors were installed on a mounting plate facing the air flow. The box was fitted with inlets in one end (front) and outlets in the other end (back) of the chamber to generate the moving air and to provide sampling air to the reference instruments. Holes were drilled in the back of the chamber to let spill air escape. The whole box was placed in a fume hood to limit human exposure to aerosols. A small fan in the mixing chamber mixed the air.

The air in the chamber was circulated from the outlet to the inlet with a pump and a

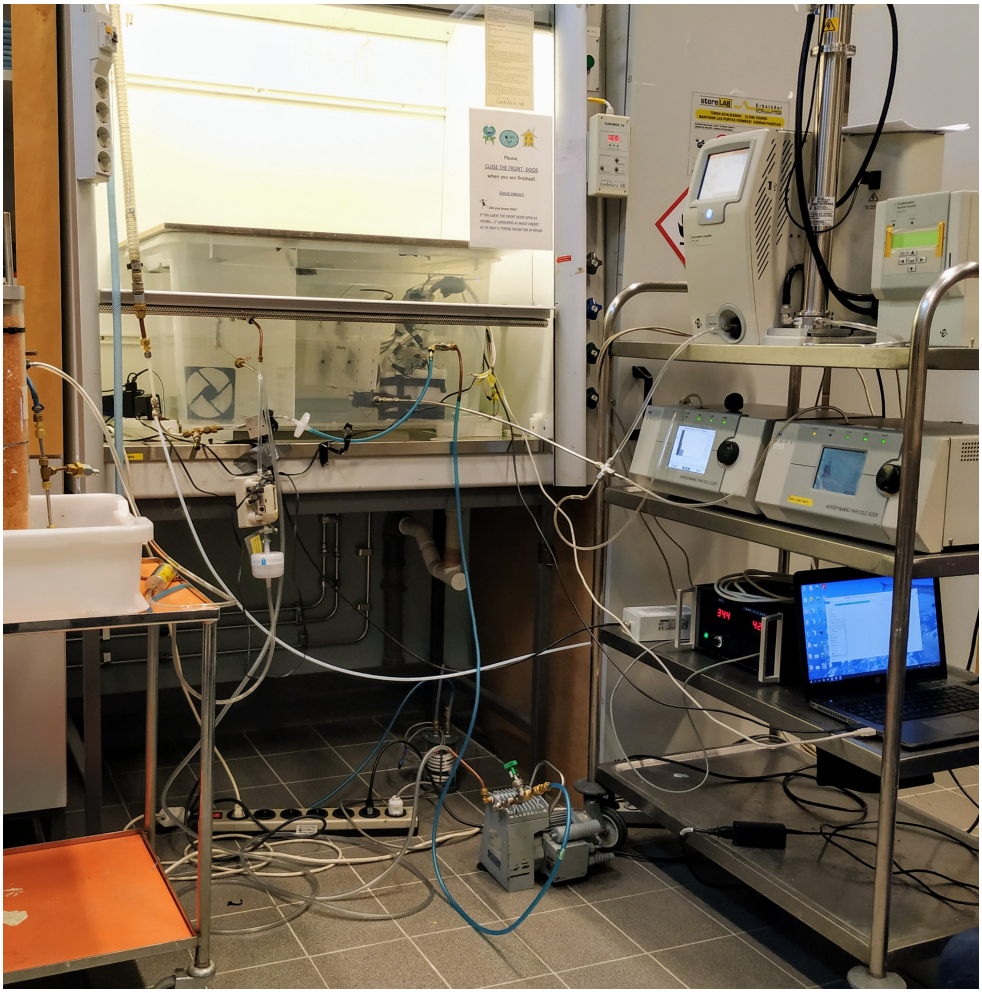

Figure 30: Picture showing the whole lab setup.

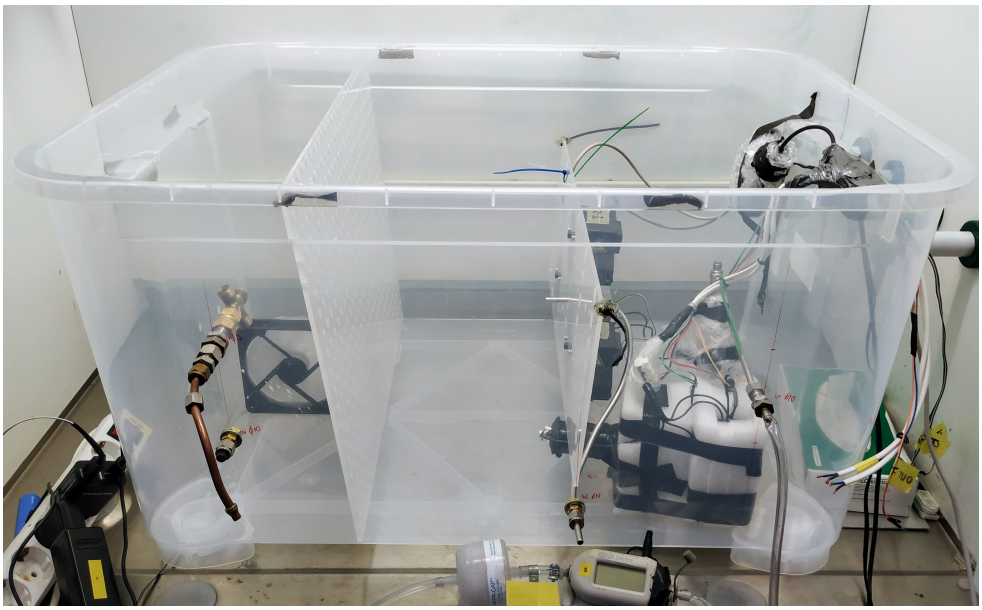

Figure 31: Close-up picture of the particle chamber

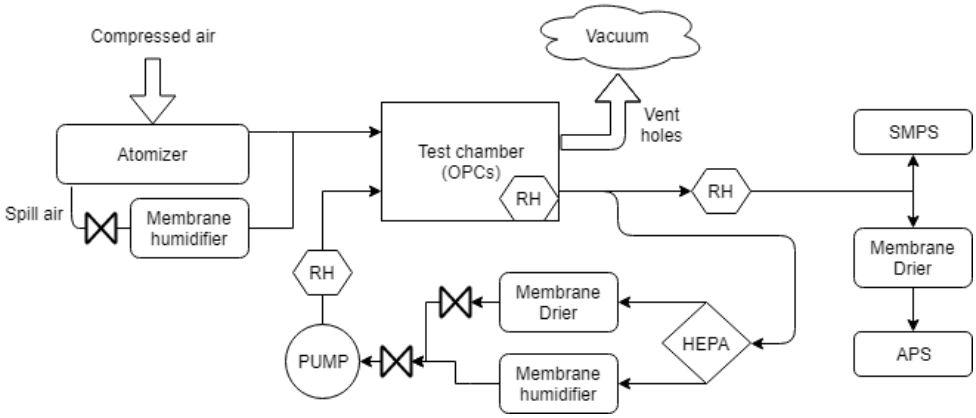

Figure 32: Diagram presenting the test chamber in the laboratory setup.

HEPA-filter in between. The circulated air could also, depending on the test case, be dried or humidified. Additionally, air containing aerosol was added to the chamber. The total air flow was max 30 l/min resulting in laminar flow ($Re < 2100$).

Figure 31 shows the complete test chamber. Figure 32 shows the diagram of the whole lab setup based on the chamber. Figure 30 presents the whole lab setup as it was used during tests.

3.5.3 Aerosol generation

Ammonium nitrate (NH_4NO_3) was used as the substrate to generate aerosols. It was chosen since it is easy to atomize and has a smaller hysteresis in its hygroscopic growth compared to other similar salts (not as state dependent). The ammonium nitrate was mixed with distilled water with a mass concentration of $1.18 \cdot 10^{-3}$.

The aerosol was generated with an atomizer that uses pressurized air to disperse a liquid substrate into small airborne particles. The aerosol concentration was controlled by adjusting the spill air valve on the atomizer. The aerosol from the atomizer was then led into the mixing chamber.

3.5.4 Drying and humidifying

A major part of the experiment concerns how the sensor readings differ with different kind of humidity levels. This was controlled by connecting a silica drier and Gore-Tex membrane humidifier to the circulated air. The humidity was then manually controlled using valves to guide the air into the drier or humidifier. Humidity sensors both in the inlet, outlet and in the chamber were used as a feedback for control and were calibrated with a dew-point generator in preparation for the experiment. When increased humidity was desired, a humidifier was also connected to the spill air on the atomizer. In addition, a wet paper towel was placed inside the chamber to reach humidity levels above 70%.

3.5.5 Instrument reading

Two reference instruments were used, an APS for measuring particles above 500 nm diameter and an SMPS for measuring below 500 nm diameter. In this setup, ammonium nitrate had a mean diameter of 60 nm and only small part of the particles were above 500 nm. The reference instruments' data can thus be combined to extract a more complete range of the particle distribution.

The reference data is supposed to sample the dry particles to avoid them being dependent on humidity. To solve this the air is dried with a Gore-Tex or silica

drier before being measured by the reference instruments. The reference instruments were monitored to always sample air below 40% humidity independent of the actual humidity in the chamber.

3.5.6 Test conditions

Two kinds of tests were performed.

- Variation of humidity - All sensors were without any heating. A constant particle concentration was attempted to be kept during the whole test. Humidity increased in steps, from dry air to moist air.
- High humidity with and without heating - Two sensors were equipped with the heating prototype. The particle concentration and humidity was attempted to be kept constant. The heating was in the beginning turned off, and then turned on.

4 Results

The statistical computer language R [9] was used to handle and plot the data from different sources. The data was modified so that they all had the same timestamp and were easy to compare to each other. Additional data handling was carried out depending on the type of plot presented.

4.1 Field test

The data from the two field tests has here been merged. This can be done since the same sensors were used. Higher levels of humidity were observed in the late winter while lower humidity was observed in the spring. The data thus complements each other. The reference by the TEOM is provided by the environmental department of Malmö Stad. The reference data is not officially verified but will here be assumed to be mostly correct.

4.1.1 Winter field test

Figure 33 show the PM2.5 time series plot from the February measurements. Big spikes can be observed from the Alphasense sensors that don't seem to be very correlated with the reference data. These spikes seem however often to be correlated with high humidity values. Another observation includes what seems like a constant offset between N2-1 and N2-2. At lower humidity (around 60%), N2-1 seems to be in line with the reference. A lower humidity than 50% was not observed during this measurement. The corresponding PM10 time plot in Figure 34 shows similar tendencies as for PM2.5.

4.1.2 Spring field test

The first days of deployment were performed without heating to measure low-humidity air. Heating was turned on the 26th of April. N2-1 initially worked but stopped outputting data about 24 hours later. The reason at the time of writing

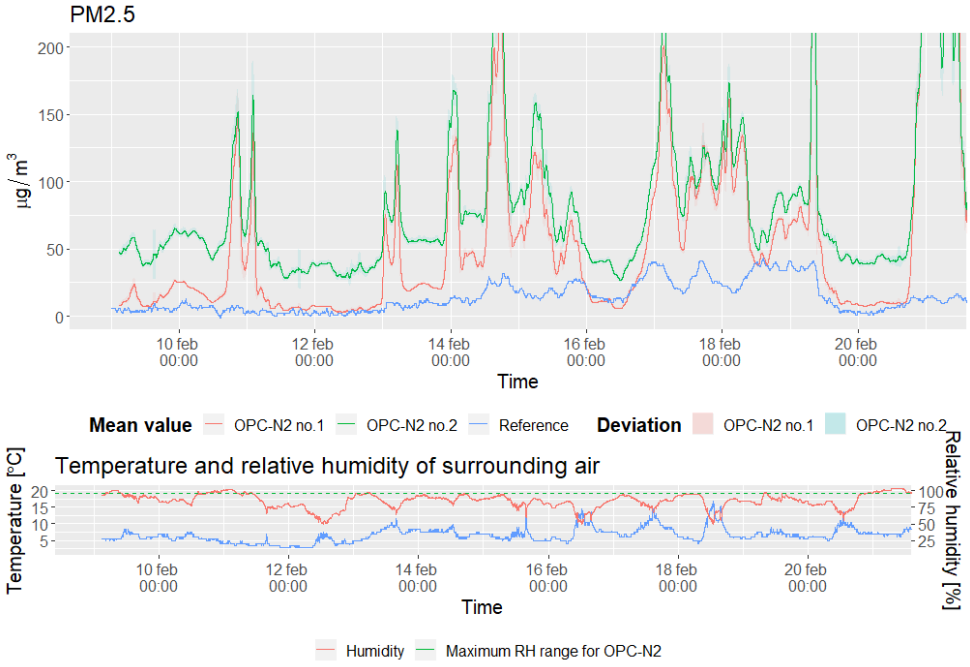

Figure 33: Figure showing mass concentration of PM2.5 from the first field test. The upper graph in the figure displays a 60-minute mean average of the PM mass concentration for N2-1 (red) and N2-2 (green) together with the reference (blue). The lower graph shows the temperature (blue) and humidity (red) for the corresponding period.

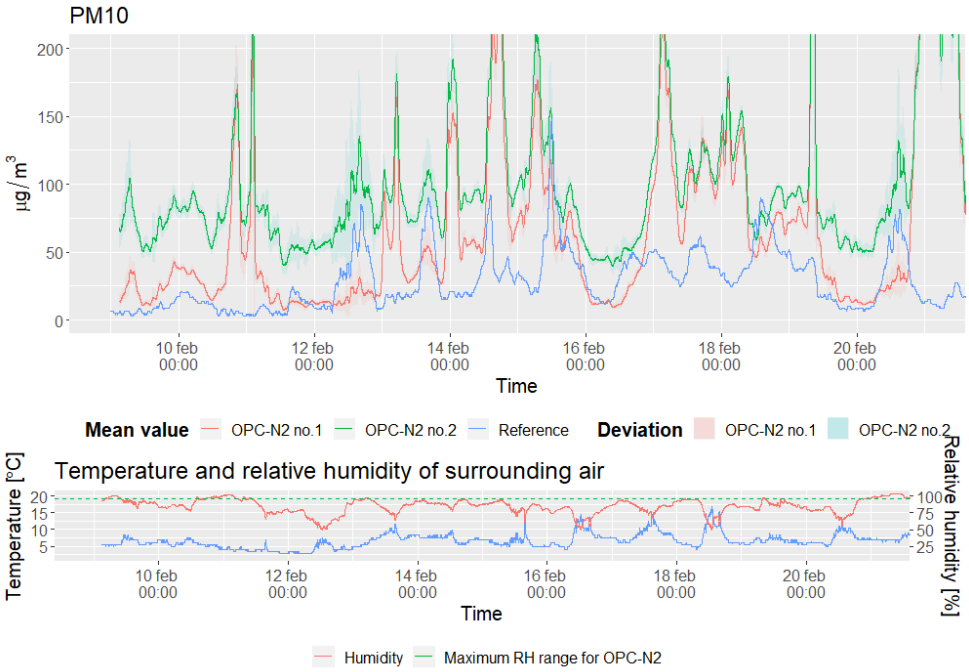

Figure 34: Figure showing mass concentration of PM10 from the first field test in same way as for Figure 33

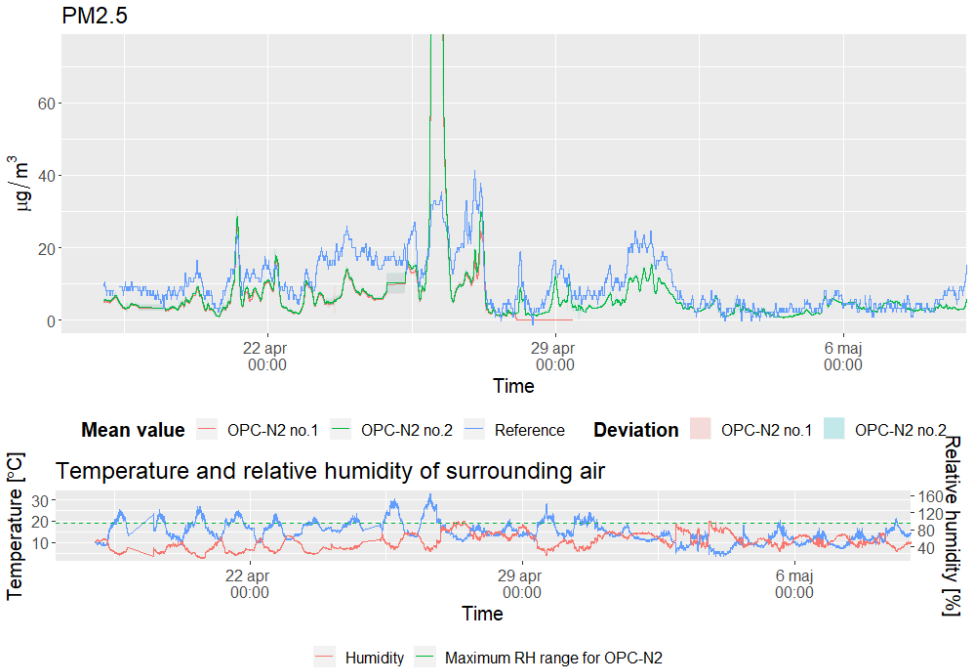

Figure 35: Figure showing mass concentration of PM2.5 from the second field test in same way as for Figure 33

is still unknown but is suspected to be due to water penetration into the box. These suspicions are strengthened by rain being present at the point of failure, and that one separate temperature sensor started showing invalid data around the same time. The software that managed the sensors also stopped working a few times but was restored within a few hours.

The time series plot for the second deployment is shown in Figure 35. An initial observation is that the values of N2-1 and N2-2 seem to be closer to both the reference and each other compared to in the previous figure. They are so close to each other that it is difficult to distinguish the two plot lines. A spike is seen at the middle of the plot for both sensors. This does not seem to be correlated with the humidity. The reference also increases but not as much. Big concentrations of desert sand from the Sahara was reported the same day of the spike which may provide an explanation [41]. The concentration showing higher than reference could be due to coincidence error (2.2.1).

The PM 10 time series plot in Figure 36 shows similar spikes, with an additional spike seen for the reference. This could perhaps be explained by the previously mentioned sand where the TEOM could have picked up some bigger particles that the Alphasense sensors didn't.

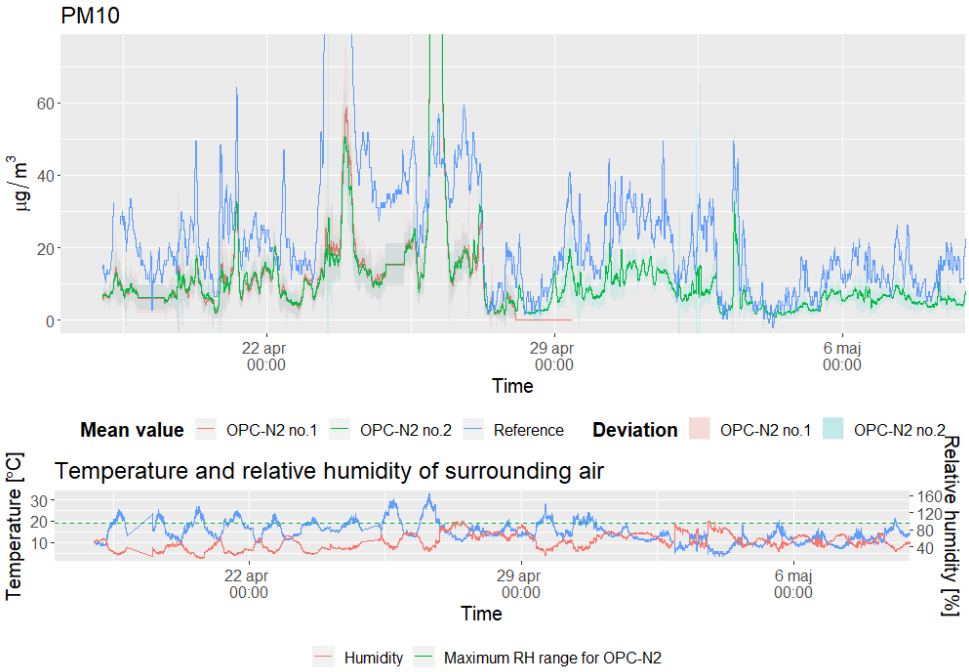

Figure 36: Figure showing mass concentration of PM10 from the second field test in same way as for Figure 33

It is in these graphs difficult to see how the data changes character when heating is turned on. This and general correlations to humidity will be further explored in upcoming graphs.

4.1.3 Without heating

Before looking at heating it is worth taking a look of how humidity is related to the measurement error. This is seen in Figure 37. The error seems to be quite constant for PM2.5 below RH 50%. For PM10 the error seems to be the least around RH 60% and RH 0%, and in between those points there seems to be a negative error. Above RH 75% the average error in all graphs increases exponentially with increasing RH. This is consistent with the fact that many particles experience an activation of absorption around this humidity. In addition, a bigger variability of error is seen with increased RH. The mean value and standard deviation is shown by the plot.

A few unusually big errors for PM10 around RH 25% are seen for both sensors. These can be traced to the spike for the reference seen in the time series plot for the spring field test.

4.1.4 With heating

All measurement points with the heating on are from the second field test. The data points from N2-1 are limited since it stopped functioning a day after heating was turned on. The result will still be presented, but more emphasis should be put on N2-2 since more data points are collected for that sensor.

Each PM value for each sensor is shown in Figure 38 and Figure 39 with the reference data plotted on the x-axis. A linear regression line and the Pearson correlation value is shown in the figures. It can be observed that the data points show less variance and are more centered around the regression line, especially for N2-2. This is also confirmed with the correlation value that shows an improvement for all sensors and PM values.

The graph with the error related to the humidity without heating is shown in Figure 37, while in Figure 40 it is shown with the heating. A big increase of error could be observed after RH 75% in the previous graphs without heating. That tendency is eliminated when heating is enabled, and the mean value and standard deviation is lowered for all cases.

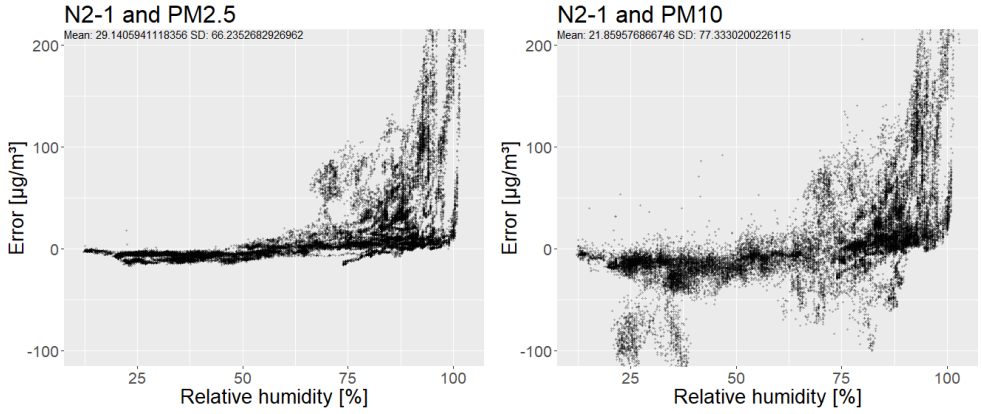

(a) N2-1 and PM2.5 without heating. Mean: 29.14, SD: 66.24

(b) N2-1 and PM10 without heating. Mean: 21.86, SD: 77.33

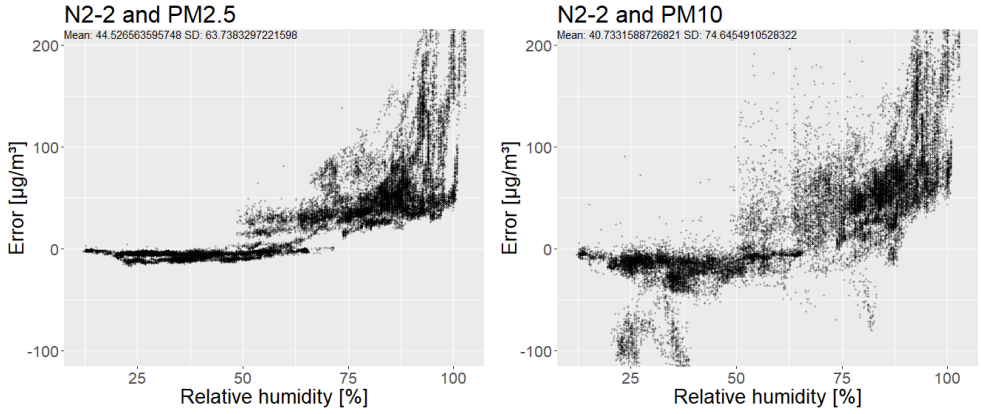

(c) N2-2 and PM2.5 without heating. Mean: 44.52, SD: 63.74

(d) N2-2 and PM10 without heating. Mean: 40.733, SD: 74.65

Figure 37: The error is for each measurement point for PM2.5 and PM10 plotted with the humidity on the x-axis, where error means the actual difference between the sensors and the reference. The heating is turned off.

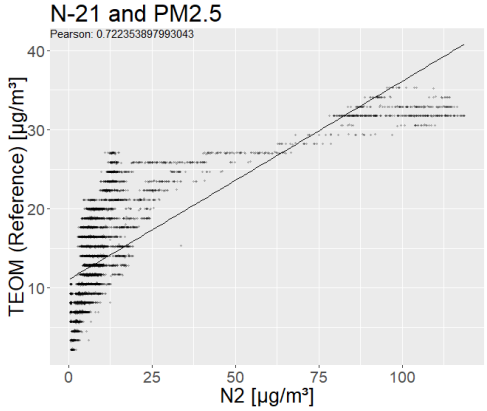

(a) N2-1 and PM2.5 without heating. Bivariate correlation: 0.722

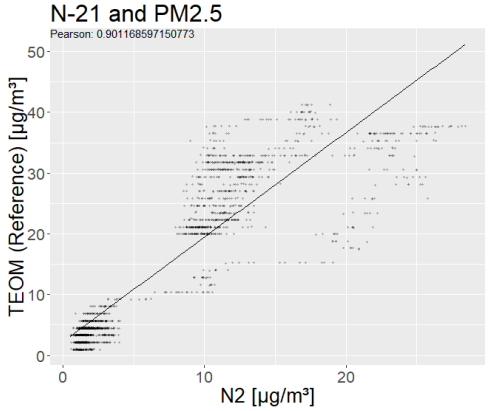

(b) N2-1 and PM2.5 with heating. Bivariate correlation: 0.901

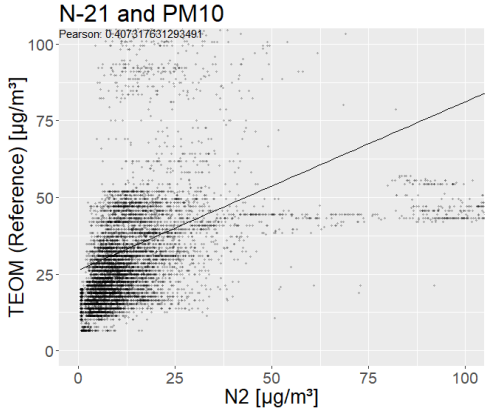

(c) N2-1 and PM10 without heating. Bivariate correlation: 0.407

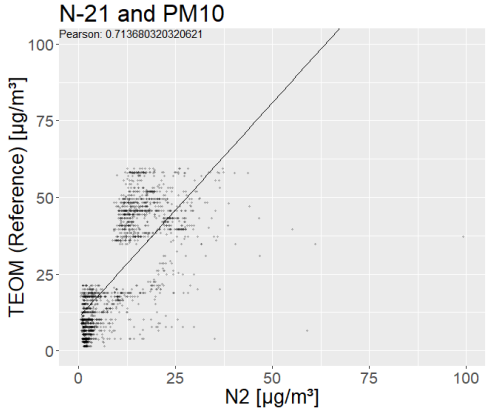

(d) N2-1 and PM10 with heating. Bivariate correlation: 0.714

Figure 38: These figures show the reference on one axis and the sensor data on the other axis for N2-1. A linear relationship between the two variables would show that the sensor data is related to the reference. A way of measuring a linear relationship is by calculating the correlation. The value of correlation goes between 0 and 1, where a higher value shows a higher linear relationship. Heating is set to heat up to RH 35%.

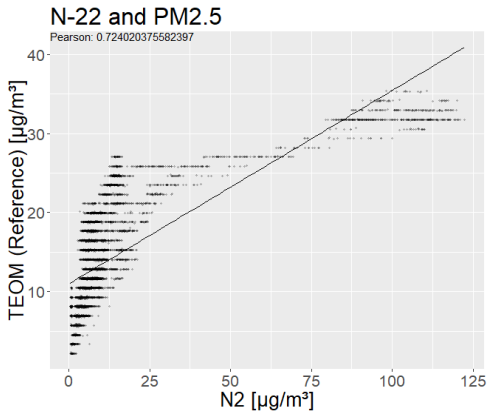

(a) N2-2 and PM2.5 without heating. Bivariate correlation: 0.724

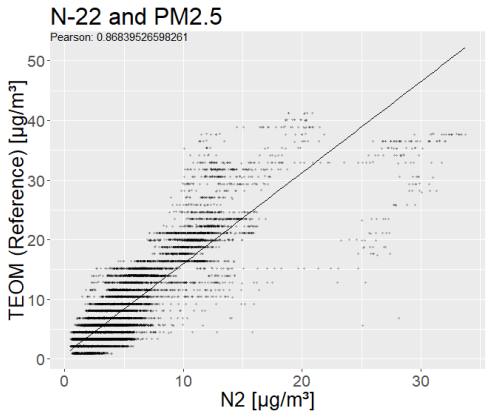

(b) N2-2 and PM2.5 with heating. Bivariate correlation: 0.869

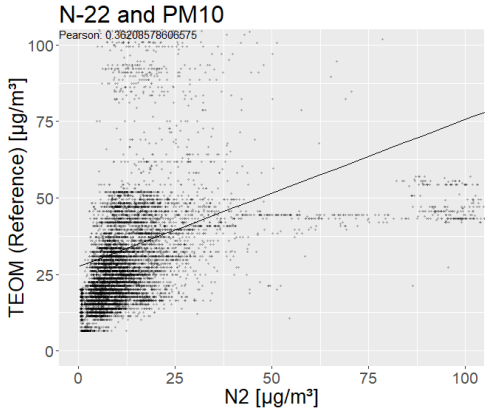

(c) N2-2 and PM10 without heating. Bivariate correlation: 0.362

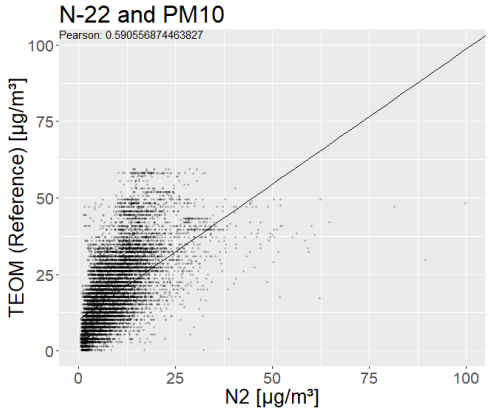

(d) N2-2 and PM10 with heating. Bivariate correlation: 0.594

Figure 39: The same graphs as in Figure 38 for sensor N2-2

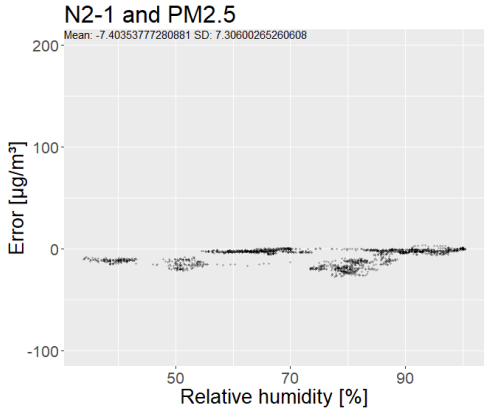

(a) N2-1 and PM2.5 with heating. Mean: -7.40, SD: 7.31

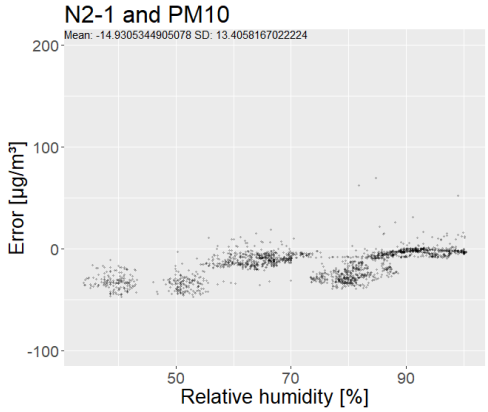

(b) N2-1 and PM10 with heating. Mean: -14.93, SD: 13.41

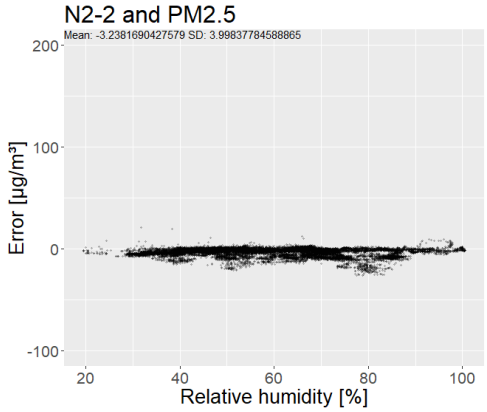

(c) N2-2 and PM2.5 with heating. Mean: -3.24, SD: 4.00

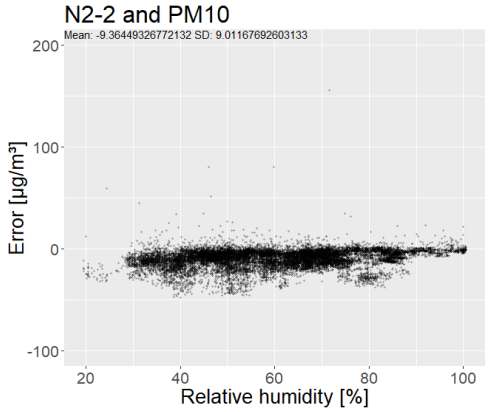

(d) N2-2 and PM10 with heating. Mean: -9.36, SD: 9.01

Figure 40: The error is for each measurement point for PM2.5 and PM10 plotted with the humidity on the x-axis, where error means the actual difference between the sensors and the reference. The heating is turned on and is set to be 35% RH.

4.2 Lab tests

The tests were performed with both the SMPS and APS as reference instruments since the size range is limited with each instrument. The APS generally measures bigger particles while the SMPS measures smaller particles. As seen in Figure 41 the major part of particles in the chamber were below the lower detectable limit for Alphasense, which is around 350 nm. Using the whole range as a reference would show tremendously bigger values than what Alphasense would show. At first, 350 nm was set as a lower limit for the reference. It was although shown from the tests that the detection efficiency was severely limited for Alphasense at these ranges. Since the major purpose of the tests was to see how the sensors would behave with variated humidity, a reference that would show around the same value as Alphasense in dry air was desired. In the end, the reference was chosen to only rely on the readings from the APS. This is motivated by the fact the APS and the OPC has a similar detection range.

All instruments that were used measures the number concentration. The values presented here will, however, be converted to mass concentration. This is because it allows easy comparison to the results from the field test.

4.2.1 Test 1 - Variation of humidity

It was desired to have the same particle concentration throughout the test to keep it as a constant variable. This was proven difficult due to the big volume in the chamber that resulted in long times to reach steady-state. Several iterations of the test were performed in an attempt to stabilize the particle concentration. The latest iteration showed more stable concentrations and will thus be presented here.

One observation that can be seen in Figure 42 is that the variability increases with increased humidity. This is seen in the field tests as well. The mass concentration from the Alphasense sensors also increases; this is expected due to increased humidity. It can however be noticed that the reference increases as well even thought it was supposed to be constant. This is because of the previously mentioned difficulties in keeping a constant particle concentration, and not due to humidity since the reference air was dried before being measured.

The plot from lab test 1 of the concentration relative to the relative humidity is shown in Figure 42. What is seen in plot in Figure 42a is mostly coherent with what's seen in the previously shown time series plot since the humidity increased with time. It can also be seen especially in plot in Figure 42b that the the error seems to be the least when it is very dry and when the relative humidity is around 60%. This was

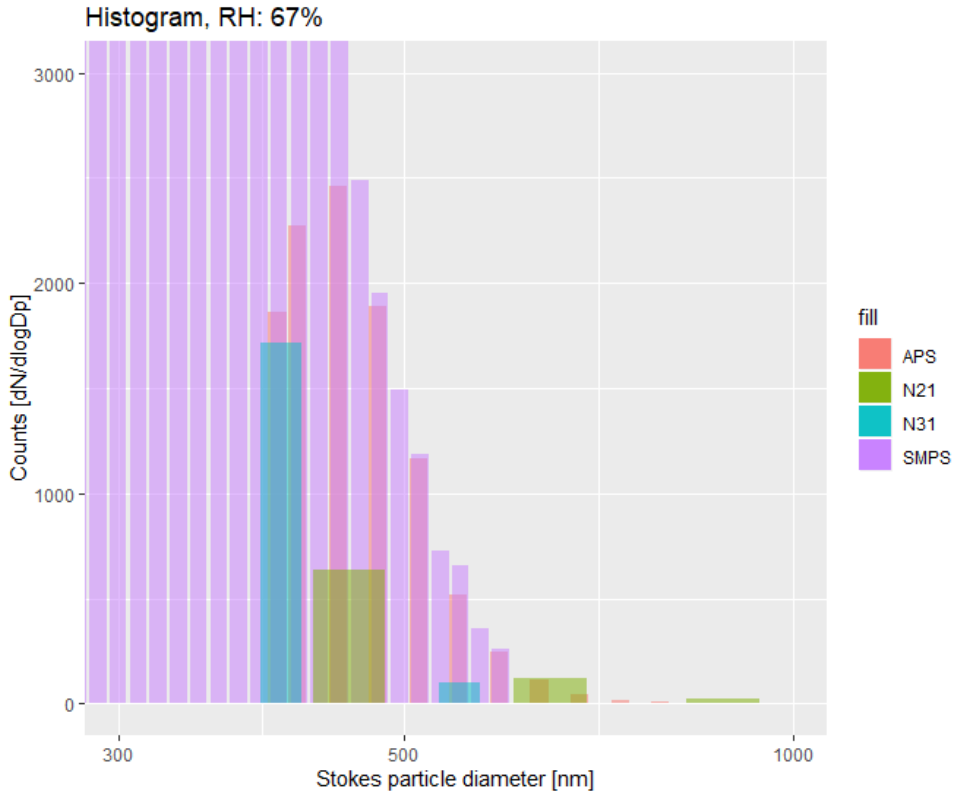

Figure 41: Histogram showing the normalized bins of particle concentration for one OPC N3 (blue) and one OPC N2 (green) together with reference data from SMPS (purple) and APS (red).

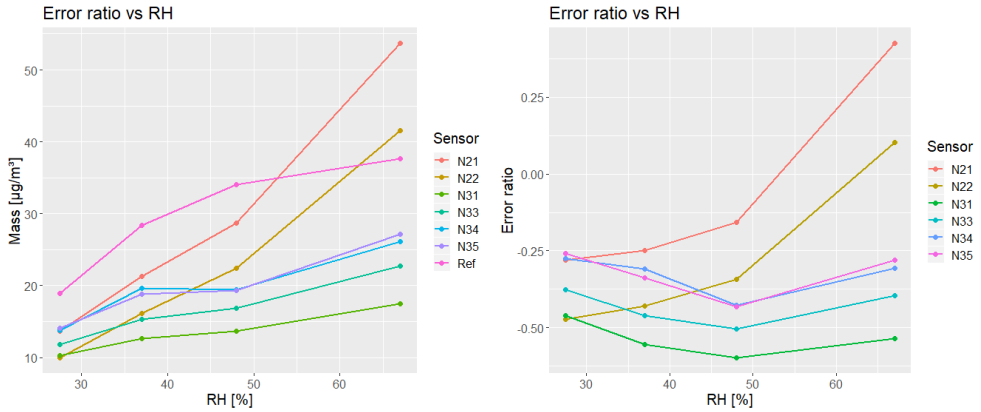

(a) Plot showing the mass concentration related to RH

(b) Plot showing the error ratio (sensor-reference)/reference related to RH.

Figure 42: Results from lab test 1. The graphs show the relation to the measured concentration and relative humidity, with two types of presentations.

also seen from the field tests.

One can also notice that the behaviour from OPC-N2 and OPC-N3 seem to differ a bit when approaching higher humidity. This seems to indicate that there are systematic differences in the measurement of particle concentrations between OPC-N2 and OPC-N3, even though they are built very similar.

4.2.2 Test 2 - High humidity with and without heating

Plot in Figure 43 shows the time plot of measured particle concentration for a constant humidity of 80%RH. The same sensors as test 1 are tested, but with added heating for N2-1 and N3-4 . The heating was turned on around 14:17 where a dip soon followed for both sensors. The concentration was here also attempted to be kept constant but was not as successful as the previous test.

The measured mass concentration in plot shown in Figure 43 decreases when heating is turned on. This is expected since the particles should dry and decrease in size. The rest of the behavior in this graph is however difficult to interpret. A possible explanation to why the heated sensors seem to have another curve than the rest of the sensors before heating could be the placement. The heated sensors were placed at the bottom of the box while the rest were placed in the center. The reference curve is also not followed very well by any sensor. This might be because of the measured increase of concentration by the APS mostly will be in the lower particle size bins, because of the particle distribution curve. These may not be measured well

by the Alphasense sensors. No conclusions regarding the effectiveness of heating is determined be made from this graph.

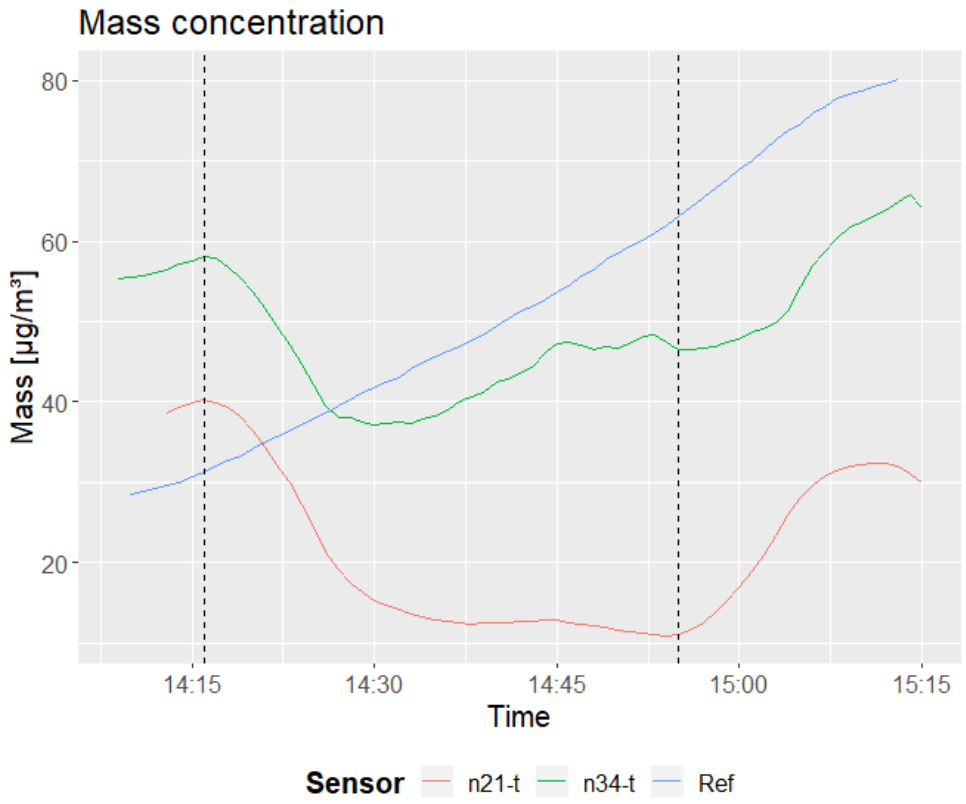

Figure 43: Time plot with a 5 minute mean average from lab test 2. The heated sensors are N2-1 (red) and N3-4 (green). The heating was turned on around 14:17 and turned off around 14:50, these timestamps are marked with dashed lines. The reference is the blue line.

5 Discussion

5.1 Field tests

The summarized results from the field test is that the humidity induced error is reduced when heating is enabled. The Pearson correlation efficient went from an average of 0.554 without heating to 0.770 with. When considering the graph plotting the error versus humidity, the average mean value and standard deviation went from 34 ± 70.49 to -8.73 ± 8.43. These numbers indicate a considerable improvement.

The sensors studied in the field tests show a big effect of relative humidity, with the error being the least around 60% and growing exponentially above 75%. Other studied have been conducted that show varied results. Wang et al. [43] noted similar behavior from their study with a Plantower PMS 7003, a low-cost PM sensor similar to the Alphasense OPC-N2. Their study showed the correlation being the highest in the middle span while being lower in the 20% and 90% range. Badura et al. [2] showed an for OPC-N2 an increased overestimation of particle concentration above 80%. Other studies such as Bulot et al. [3] noted with OPC-N2 no big effect from relative humidity. The varied results show that other factors may also influence the result. One factor that was not properly explored in this thesis is how the particle concentration influences the error in relation to relative humidity. This might be one reason why different studies show different results.

When looking at the correlation before and after heating, the different measurements were done at different times. The major part of the data points without heating was conducted in February, where humidity generally was higher. All data point with heating were done in the Spring, where humidity was lower. It is thus likely that the correlation would be higher for the plot with heating, even if heating would never have been switched on. The quantitative correlation factor is to be taken with a grain of salt. However, there were also periods where high humidity and rain was present even for the data points with heating on. These would show up as large deviations in the plot but are not present. A higher correlation with the reference with heating is thus still valid. More caution would have to be made if these deviations were seen in the chart. A suggestion for improvement to avoid this error source all together is to collect data points close in time to each other. This could have been implemented by switching the heating on and off in periods, as to collect data point close in time.

This was discussed but not implemented since it was uncertain how long time it would take for the sensors to heat up and cool down. Another possibility would be to look at the correlation only for high humidity. This is possible with the current data, but was not done due to time constraints.

5.2 Lab tests

There were difficulties in generating larger particles. Most of the particles put in the box were smaller than what Alphasense according to its specifications could detect. A suspicion is that this may have attributed to some results being hard to interpret. Having most particles being larger than the Alphasense detection limit would remove an error source attributed to different detection limits for the reference instruments and Alphasense.

It was not completely certain what to look for before the experiment was conducted, and the goal was that additional information could be collected by being able to vary certain variables. In the end, having a low amount of data points made the data appear as low-resolution compared to the field tests. It can be argued that having field tests alone would have been sufficient for this thesis.

5.3 Solution

The prototype solution was deemed successful in its goal of reaching the specifications set up. The most important task was in successfully heating the air, which was archived. The solution was easy, which made it easy to make but also cheap. The cost was estimated to be less than 1000 SEK but can be reduced further by optimizing the design.

Heating was implemented both in the pipe and around the sensor. This was done to avoid the risk of air cooling while being inside the sensor, thus having the relative humidity increase again. For further improvement it should be investigated if one of these heat sources could be removed; either the heating around the sensor or perhaps even heating of the pipe itself. Another aspect regarding the construction of the heating is the pipe length itself. When a laminar flow enters a pipe, the air has more contact with the wall in its entrance region until reaching it's fully developed flow [44, p. 277]. A hypothesis could thus be made that the most heat exchange

due to convection will occur at the pipe entrance since a no-slip condition has not occurred yet for the fluid. Another aspect of the pipe length is disturbance of the flow rate, the flow rate test were done on an OPC-N3 unit, see Appendix A; however the effects of the flow rate on PM reading remain unknown. Optimization of pipe length was not included in this thesis but might become relevant if the length of the pipe is a limiting factor for an application.

There have been several attempts in studies to compensate for the humidity error theoretically. Di Antonio et al. [8] recently published a study that uses the particle composition to theoretically compensate for humidity, where a relative error of 5 was reduced to 1.05. Such a working solution would probably provide an easier and cheaper implementation. It is although worth measuring that such compensations have to make assumptions about the particles in the air. This is not required when removing the humidity physically.

The current prototype is quite big which may become an issue in many applications. Another problem is that it consumes quite a bit of power. Further work in development this solution includes optimization of these factors.

6 Conclusions

It has in this study been shown that Alphasense OPC-N2 are susceptible to humidity induced errors, especially when the relative humidity goes above 75%. Implementing a heated inlet reduced this error significantly in the field test and presented an increased correlation between the sensors and the reference. The data from the laboratory test is difficult to comprehend, and any results about the effectiveness of heating are deemed inconclusive from this test alone. A general conclusion is that heating is a technically simple solution that helps in reducing humidity induced errors.

Further work regarding heating as a compensation method includes optimization of the heated inlet in terms of reducing its size and energy consumption.

A Flowrate test of an OPC-N3

Since the heated inlet developed in this thesis uses a pipe attached to the sensor's inlet, a flow rate test was done to see if different tube lengths affect the airflow of the OPC-N3 sensor.

The flowrate of the OPC was tested by attaching it to a Gilibrator-2 bubble generator with various lengths of Tygon tubing with an inner diameter of 5mm. Table 44 presents the results of this test, the flow rate is an average of five measurements point.

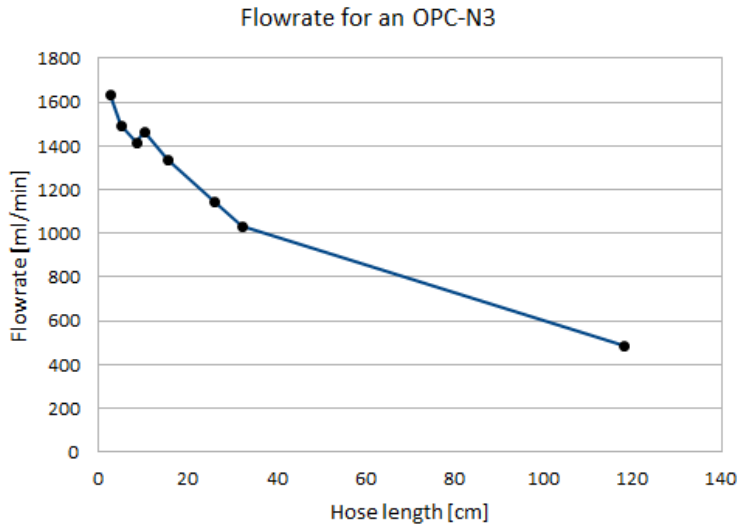

Figure 44: Results of a flow rate test of an OPC-N3

As it can be seen in the results the maximum measured flow rate was $1.6l/min$ with a $2,5cm$ tube. The flow rate drops with longer tubes as it was expected. With the tube length of $15,5cm$, which is as long as the heater pipe, the flow rate dropped down to $1,34l/min$. This drop should be smaller with an 8mm inner diameter pipe that was used in the heater prototype. With this and the limited scope of this thesis in mind, it seems reasonable to neglect OPC flow rate drop caused by the heater.

However, the effect of the tube and pipe length on the measurement of particles should be studied in more detail in future work.

B Properties for the air conditioner

Table 5: Target properties for the prototype. Similar as in [42, Fig. 6.4]

Index	*Need index*	*Quality*	*Weight*	*Unit*	*Acceptable value*
1	1	Can reach specified moisture content	5	RH%	<30
2	2	Needs manual calibration for different settings with different kind of particles	3	Yes/No	No
3	3	Static buildup	4	-	None
4	3	Little particle loss within evaluated spectrum (PM1-PM10)	4	Yes/No	Yes
5	4	Reynolds constant in front of inlet	5	-	<2100 (laminar)
6	4	Pressure loss	5	Pa	<40
7	4	Inlet direction	5	-	Up/down
8	5	Energy efficiency	2	%	>20
9	6	Length (upwards)	3	Cm	<20
10	6	Diameter	3	cm	<6,5
11	7	Cost	4	SEK	<3000
12	8	Low complexity	3	Yes/No	Yes
13	9	Voltage in circuit	5	V	<12
14	9	Redundant safety systems	5	Nbr	>2
15	10	Needs constant upkeep	4	Yes/No	No
16	11	Easy to install	4	Yes/No	Yes
17	12	Can be adapted for different kind of sensors	3	Yes/No	Yes
18	13	Weather proof	5		Yes

C Electronic components

C.1 SPI multiplex board

The custom board was designed to allow the selection of up to four SPI devices. Board was designed to be attached to a RPi with general purpose input-output (GPIO) and a micro USB cable. Power can be supplied to the board which distributes it to the RPi and four connectors to SPI devices.

The board was based on two integrated circuits (ICs). First IC was a quadruple bus buffer gate(SN74HC125N)[20] from Texas Instruments which function was to connect and disconnect RPi's master in, slave out (MISO) line from the SPI device. The second IC was a 2 to 4 line decoder(SN74HC139N)[19] also from Texas Instruments. The decoder translates RPi's binary output and activates correct MISO channel on the buffer IC. The complete board schematics can be found in figure 45.

C.2 OPC control board

Custom board designed to connect with an Alphasense OPC-N2 or OPC-N3 PM sensor over the SPI, communicate with the RPi over a serial port and control two heaters.

The board was based on an Arduino Pro Mini compatible development board [21] with an ATmega328p MCU running at 8Mhz and powered by 3.3V. Simple On-Off controller was implemented on the MCU to control pulse width modulation (PWM) pins output. Feedback to the controller is provided by two NTC thermistors which read the temperature of the heaters. The PWM output pins control two metal–oxide semiconductor field-effect transistors (MOSFETs) supplied with 12V which allows to regulate the temperature of the heaters.

Code written for the board listens to text commands sent to it over the serial port, performs the task and sends the answer back. While waiting for commands the heater controller code is executed and a histogram from the OPC is polled. The board uses SPI to communicate with the OPC-N2 by exchanging byte sequences. An already existing C++ library for Alphasense OPC-N2 for Arduino [45] was adopted.

The complete board schematics can be found in figure 46.

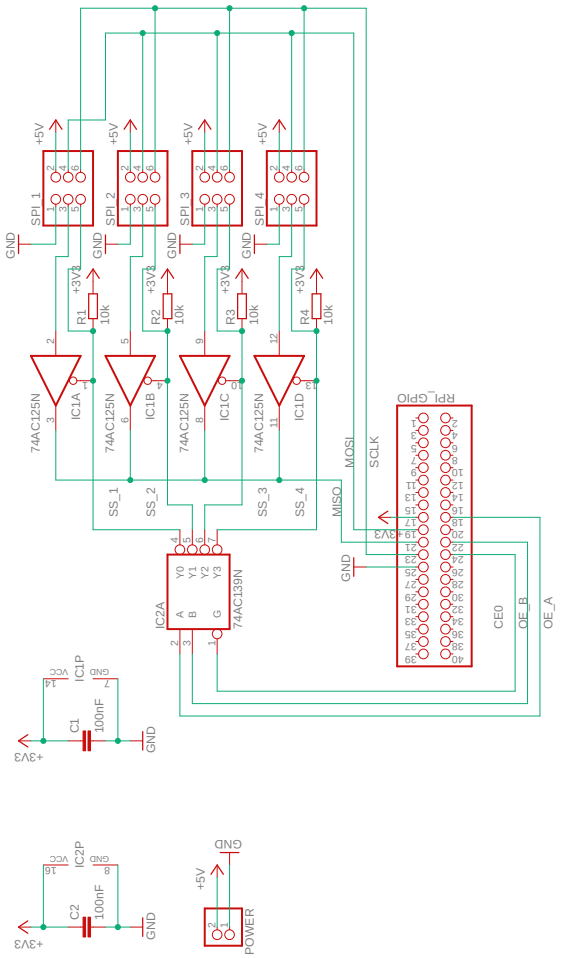

Figure 45: Schematics of the SPI selector board.

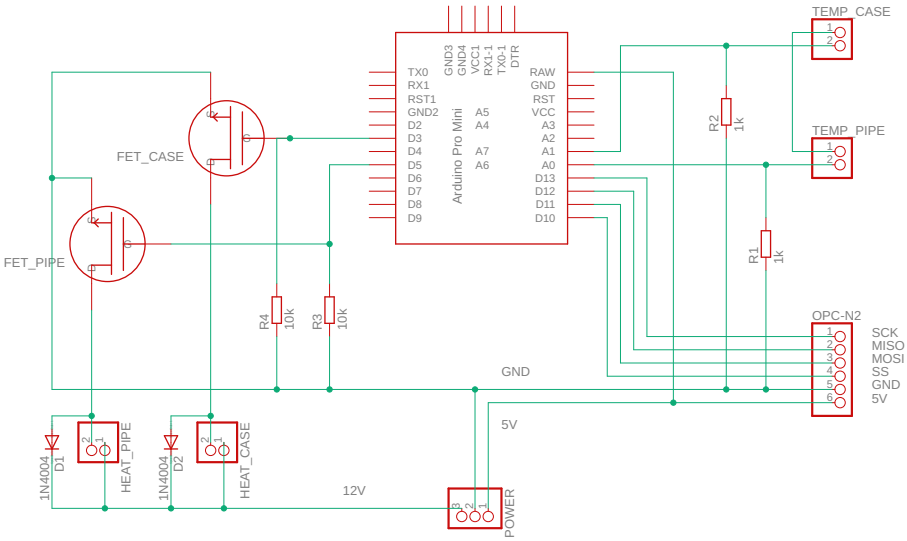

Figure 46: OPC control board schematics.

C.3 NTC thermistors

Negative temperature coefficient thermistors are electrical components that decrease their resistance while temperature rises. Thermistors used in the thesis had value of $10k\Omega$ and were connected in a voltage divider configuration to the microcontroller's analog-to-digital converter (ADC) input.The measured resistance of the thermistor was then converted by MCU into temperature with the help of Steinhart-Hart equations [39].

C.4 Humidity and Temperature Sensor - Si7021

SparkFun breakout board features Silicon Labs Si7021 chip which is a combined humidity and temperature sensor. The sensor can communicate with other devices

over the I^2C bus. Some important features taken from this sensor's datasheet [13] are:

- Precision Relative Humidity Sensor ±3% RH (max), 0–80% RH
- High Accuracy Temperature Sensor ±0.4 °C (max), –10 to +85 °C
- RH operating range from 0 to 100% RH
- Temperature operating range from –40 to +125 °C
- Factory-calibrated
- Excellent long term stability
- Excludes liquids and particulates

D Contributions

The workload of this thesis was spread evenly between the authors. All decisions and conclusions were the result of teamwork.

References

[1] European Environment Agency. *National Emission Ceilings Directive*. URL: https://www.eea.europa.eu/themes/air/national-emission-ceilings (visited on 2019-05-27).

[2] Marek Badura et al. "Evaluation of Low-Cost Sensors for Ambient PM2.5 Monitoring". In: *Journal of Sensors* 2018 (2018).

[3] Florentin M. J. Bulot et al. "Long-term field comparison of multiple low-cost particulate matter sensors in an outdoor urban environment". In: *Scientific Reports* 9.1 (2019), p. 7497.

[4] University of Manchester Centre for Atmospheric Science. *Aerodynamic Particle Sizer*. URL: http://www.cas.manchester.ac.uk/restools/instruments/aerosol/aps/ (visited on 2019-06-03).

[5] Chen-Chia Chen et al. "Calibration of Low-Cost Particle Sensors by Using Machine-Learning Method." In: *2018 IEEE Asia Pacific Conference on Circuits and Systems (APCCAS)* (2018), p. 111. ISSN: 978-1-5386-8240-1.

[6] L. R. Crilley et al. "Evaluation of a low-cost optical particle counter (Alphasense OPC-N2) for ambient air monitoring". In: *Atmospheric Measurement Techniques* 11.2 (2018), pp. 709–720.

[7] Piyu Dhaker. *Introduction to SPI Interface*. Sept. 2018. URL: https://www.analog.com/en/analog-dialogue/articles/introduction-to-spi-interface.html# (visited on 2019-05-22).

[8] Andrea Di Antonio et al. "Developing a Relative Humidity Correction for Low-Cost Sensors Measuring Ambient Particulate Matter". In: *Sensors* 18.9 (2018).

[9] The R Foundation. *What is R?* URL: https://www.r-project.org/about.html (visited on 2019-06-12).

[10] CTS GmbH. *Climatic Test Cabinets, Series C*. URL: https://www.cts-umweltsimulation.de/en/products/climate-c.html (visited on 2019-06-03).

[11] David H hagan. *Python wrapper for the Alphasense OPC-N2 built around py-spidev*. 2015. URL: https://github.com/dhhagan/py-opc.

[12] William C. Hinds. *Aerosol technology : properties, behavior, and measurement of airborne particles*. Wiley, 1982.

[13] Silicon Laboratories Inc. *I2C Humidity and Temperature Sensor*. Si7021-A20. Available at https://cdn.sparkfun.com/assets/b/1/b/8/5/Si7021-A20.pdf. 2016.

[14] TSI Inc. *DIFFUSION DRYER 3062*. URL: https://www.tsi.com/product-accessories/diffusion-dryer-3062/ (visited on 2019-05-28).

[15] TSI Inc. *HEATED INLET SAMPLE CONDITIONER WITH AUTOZERO MODULE 801850*. URL: https://www.tsi.com/product-accessories/heated-inlet-sample-conditioner-with-autozero-module-801850/ (visited on 2019-05-28).

[16] TSI Inc. *Model 3321 Aerodynamic Particle Sizer Spectrometer*. URL: http://fy.chalmers.se/OLDUSERS/molnar/lectures/Measurement%20Methods%20II-filer/APS-3321.pdf (visited on 2019-06-03).

[17] TSI Inc. *Model 3772/3771 Condensation Particle Counter*. URL: https://wmo-gaw-wcc-aerosol-physics.org/files/cpc_3772-3771.pdf (visited on 2019-06-03).

[18] TSI Inc. *Scanning Mobility Particle Sizer Spectrometer Model 3938*. URL: https://www.tsi.com/getmedia/3705a532-8dd8-46eb-832d-0bce6ab2921b/SMPS-3938_A4_5001532_RevE_Web?ext=.pdf (visited on 2019-06-03).

[19] Texas Instruments. *Dual 2-line to 4-line Decoder/Multiplexer*. SN74HC139N. Available at https://www.ti.com/lit/ds/symlink/sn74hc139.pdf. Dec. 1982.

[20] Texas Instruments. *Quadruple Bus Buffer Gates With 3-State Outputs*. SN74HC125N. Available at https://www.ti.com/lit/ds/symlink/sn74hc125.pdf. Aug. 1984.

[21] *Köp Pro Mini 3.3V 8 MHz MEGA328 till rätt pris @ Electrokit*. URL: https://www.electrokit.com/produkt/pro-mini-3-3v-8-mhz-mega328/ (visited on 2019-03-25).

[22] Pramod Kulkarni, Paul A. Baron, and Klaus Willeke. *Aerosol measurement: principles, techniques, and applications*. Wiley, 2011.

[23] *Kvalitetssäkringsprogram för Samverkansområdet Skåne*. Apr. 2019.

[24] Alphasense Ltd. *Alphasense User Manual OPC-N2 Optical Particle Counter*. English. Version 5. Dec. 2015. 34 pp.

[25] Alphasense Ltd. *Alphasense User Manual OPC-N3 Optical Particle Counter*. English. Version 1. Aug. 2018. 31 pp.

[26] D. A. Lundgren and D. W. Cooper. “Effect of Humidify on Light-Scattering Methods of Measuring Particle Concentration”. In: *Journal of the Air Pollution Control Association* 19.4 (1969), pp. 243–247.

[27] Naturvårdsverket. *Fakta om partiklar i luft*. URL: https://www.naturvardsverket.se/Sa-mar-miljon/Klimat-och-luft/Luftfororeningar/Partiklar/ (visited on 2019-06-03).

[28] Naturvårdsverket. *Webbtjänst luftkvalitetsdata*. URL: http://www.naturvardsverket.se/Sa-mar-miljon/Klimat-och-luft/Statistik-om-luft/Webbtjanst-luftkvalitetsdata/ (visited on 2019-05-21).

[29] Carl R. (Rod) Nave. *Relative Humidity*. URL: http://hyperphysics.phy-astr.gsu.edu/hbase/Kinetic/relhum.html (visited on 2019-02-22).

[30] *Nova PM sensor SDS011*. URL: https://www.lawicel-shop.se/nova-pm-sensor-sds011 (visited on 2019-05-27).

[31] World Health Organization. *Air Pollution*. URL: https://www.who.int/airpollution/en/ (visited on 2019-05-27).

[32] World Health Organization. *Guidelines*. URL: https://www.who.int/airpollution/guidelines/en/ (visited on 2019-05-27).

[33] Jayaratne R. et al. “The influence of humidity on the performance of a low-cost air particle mass sensor and the effect of atmospheric fog.” In: *Atmospheric Measurement Techniques* (2018), p. 4883.

[34] Magee Scientific. *DIFFUSION DRYER 3062*. URL: https://mageesci.com/our-products/inlet-dryer/ (visited on 2019-05-28).

[35] Thermo Scientific. *8500 Filter Dynamics Measurement System*. URL: https://www.thermofisher.com/order/catalog/product/8500 (visited on 2019-03-25).

[36] Thermo Scientific. *Continuous Ambient Particulate TEOM^{TM} Monitor, Series 1400ab*. URL: https://www.thermofisher.com/order/catalog/product/1400AB (visited on 2019-05-21).

[37] Thermo Scientific. *TEOM Technology for Particulate Matter Measurement*. URL: https://www.thermofisher.com/se/en/home/industrial/environmental/environmental-learning-center/air-quality-analysis-information/teom-technology-particulate-matter-measurement.html (visited on 2019-06-03).

[38] S. P. Silva et al. “Cork: properties, capabilities and applications.” In: *International Materials Reviews* 50.6 (2005), pp. 345–365.

[39] John S. Steinhart and Stanley R. Hart. “Calibration curves for thermistors”. In: *Deep Sea Research and Oceanographic Abstracts* 15.4 (1968), pp. 497–503.

[40] B. Svenningsson et al. “Hygroscopic growth and critical supersaturations for mixed aerosol particles of inorganic and organic compounds of atmospheric relevance”. In: *Atmospheric Chemistry and Physics* 6.7 (2006), pp. 1937–1952.

[41] TT. *Sand från Sahara orsakar dis i södra Sverige*. URL: https://www.svt.se/nyheter/inrikes/sand-fran-sahara-orsakar-dis-i-sodra-sverige (visited on 2019-06-03).

[42] Karl T. Ulrich and Steven D. Eppinger. *Produktutveckling : konstruktion och design.* Studentlitteratur, 2014.

[43] Kan Wang et al. “Evaluating the feasibility of a personal particle exposure monitor in outdoor and indoor microenvironments in Shanghai, China”. In: *International Journal of Environmental Health Research* 29.2 (2019), pp. 209–220.

[44] Donald F. Young et al. *Introduction to fluid mechanics.* Wiley, 2011.

[45] Marcelo Yungaicela. *C++ Library for the Alphasense OPC-N2 particle counter-Arduino*. May 2017. URL: https://github.com/MarcelloYung/opcn2-Arduino.